PHI ZETA

The Honor Society of Veterinary Medicine
Epsilon Chapter

November 7, 2018

Research Emphasis Day

AUBURN UNIVERSITY
COLLEGE OF VETERINARY MEDICINE

PHI ZETA
EPSILON CHAPTER
COLLEGE OF VETERINARY MEDICINE
AUBURN UNIVERSITY

Welcomes you to our

PHI ZETA RESEARCH DAY FORUM
November 7, 2018

We want to thank all the presenters, their co-investigators and mentors for their participation in this annual event.

We also want to thank all sponsors for their generous support without which this event would not be possible:

zoetis

Office of the Dean
Office of the Assoc. Dean for Research and Graduate Studies
Auburn University Research Initiative in Cancer
Department of Anatomy, Physiology, and Pharmacology
Department of Clinical Sciences
Department of Pathobiology
Scott-Ritchey Research Center

PHI ZETA RESEARCH DAY FORUM

NOVEMBER 7, 2018 – VETERINARY EDUCATION CENTER

8:45: Opening Statement

Dr. Frank F. Bartol, Alumni Professor and Associate Dean for Research & Graduate Studies, Auburn University College of Veterinary Medicine

9:00-11:12 MORNING Presentations - Overton Auditorium

Veterinary Students:

9:00	Jeremy George	HPLC Method Development for Detection of Two Endocannabinoids; Anandamide (AEA) and 2-Arachidonylglycerol (2-AG) in Dog Plasma
9:12	Brandon Weyhing	Obesity in Mice: Acute vs. Chronic Effects of High-Fat Diet Feeding
9:24	Elizabeth Manson	Commensal metabolites facilitates allergen-induced dendritic cell activation and inflammation
9:36	Matthew Miller	Localization and Quantification of Cannabinoid Receptors in Canine Tissue
9:48	Jonathan Tubbs	Evaluation of semen production in boars given an IAV-S vaccine
10:00	Hannah Himmelmann	Decreasing radial contact area results in a higher coefficient of friction on articular cartilage

Graduate Students:

10:12	Sara Collins	Normal Electrocardiogram of Conscious Bald Eagles (Haliaeetus Leucocephalus)
10:24	Jeff Daniel	Characterization and functional analysis of the putative calcium-binding protein, ankef1
10:36	Amanda Gross	Intravenous delivery of AAV gene therapy in GM1 gangliosidosis
10:48	Jack Kottwitz	*In Vitro* and *Ex Vivo* Cylco-oxygenase Inhibition by Flunixin Meglumine and Firocoxib in the Asian Elephant (*Elephas maximus*)

11:00 Joy Goodwin Lecture-101 VEC

12:00–1:00 POSTER Presentations-VEC Lobby

1:00-2:45 AFTERNOON Presentations - Overton Auditorium

Graduate Students (continued)

1:00	Anne Maguire	Current Image Analysis Techniques to Quantify Adipocyte Area
1:12	Francesca Mowry	Angiotensin II, the innate immune system, and blood-brain barrier disruption in neurogenic hypertension
1:24	Damien Ruiz	Development of Oncolytic Adenovirus Library Displaying Synthetic Nanobodies in Place of Fiber Knob
1:36	Ana Velloso Alvarez	Comparison of the cytokine and cellular profile of autologous protein solution, autologous conditioned serum, and serum incubated for 24 hours in healthy horses
1:48	Ramon Zegpi	Age of Vaccination Influences Infectious Bronchitis Virus Cross-Protection

Faculty:

2:00	Lindsey Boone	Effect of 3% chloroprocaine on onset of analgesia after application of high regional nerve blocks on naturally lame horses
2:12	John Schumacher	A Comparison of General Anesthesia with Sedation and Local Anesthesia for Castration of Dogs: a Preliminary Study
2:24	Lindsey Boone	Sodium bicarbonate speeds and potentiates anesthesia of median and ulnar nerve blocks performed with mepivacaine

2:45 -3:15 Break and Snack - VEC Lobby

3:15-4:00: View Posters - VEC Lobby

4:00 KEYNOTE LECTURE-Overton Auditorium

5:00 INDUCTION AND AWARDS ANNOUNCEMENT

INDUCTION of new Phi Zeta Members

AWARD presentation

5:30 RECEPTION - VEC Lobby

PHI ZETA KEYNOTE SPEAKER AND JOY GOODWIN LECTURER

"The ABC's of Veterinary Medical Research"

Katrina L. Mealey
Richard L. Ott Endowed Chair Professor
Director, Program in Individualized Medicine
College of Veterinary Medicine
Washington State University

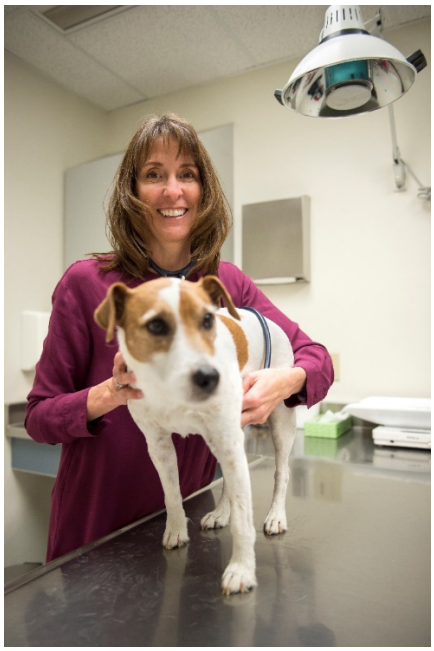

Katrina L. Mealey, Ph.D., D.V.M., is the Richard L. Ott Professor in Small Animal Medicine and Research and founding director of the Program in Individualized Medicine at Washington State University. Mealey is recognized as a global expert in veterinary pharmacogenetics because her research has changed the standard of care in veterinary medicine and has influenced veterinary drug development and regulation. She is the recipient of Eli Lilly Award, Pfizer Award for Veterinary Research Excellence, Life Sciences Northwest Women-to-Watch Award, 2018 Washington State University Woman of the Year and a Fellow of the National Academy of Inventors. She holds two U.S. patents and eight international patents that have been licensed to nine different companies. She has published over 100 peer-reviewed research articles, numerous book chapters and a book. Mealey is a diplomate of ACVIM and ACVCP and is currently the Associate Dean for Research for the College of Veterinary Medicine at Washington State University.

Posters

Undergraduate Students

Hannah Harris	Identification of Circulatory microRNA in Canine Cancer Patient Liquid Biopsies
Mackenzie Michaels	Environmental Sampling for *Salmonella* in an Equine Reproduction Center

Veterinary Students

Brooke Alnwick	Lipopolysaccharide Priming of Equine Mesenchymal Stem Cells
Natalie Heape	Arming a conditionally replicating canine adenovirus (ICOCAV15) with canine *mda-7* for cancer therapy
Amanda Hill	Effects of Auditory Environment on Dogs during Abdominal Ultrasound Examination
Brooklyn Isaacs	Mutational analysis of the Factor XIIIa gene in a Poodle with Factor XIII deficiency
Samantha Weatherford	A Case of Necrotizing Purulent Pleuropneumonia in a White-tailed Deer
Krista Wood	Cannabinoid Receptor Quantification in Normal and GM1 affected Feline Tissues

Graduate Students

Erfan Chowdhury	A Synopsis of Neoplasms Diagnosed in Backyard Chickens Submitted to the Alabama Department of Agriculture and Industries Veterinary Diagnostic Laboratory System, 2016-2017
Taylor Flaat	Evaluation of two methods to collect canine melanocytes
Christina Hargis	High Performance Liquid Chromatography-UV Detection and Validation of Primaquine phosphate in Penguin Plasma
Bamidele Jeminiwa	Effects of soy isoflavones on Leydig cell steroidogenesis
Gisela Martinez-Romero	Flow cytometry analysis of Mammaglobin-A in canine mammary tumor cell lines
Keiko Murakami	Tonsillar biopsy for routine staging of non-tonsillar primary oral tumors: Assessment of complications and evidence of disease in 28 cases

Sophonie Omeler	Complexities of familial cancer risk - investigating a large African American family
Saba Omer	Expression of cannabinoid receptors in human prostate cancer cell lines: A novel pharmacologic target?
Abdul Mohin Sajib	CRISPR-CAS9 Mediated Genetic Modification of Canine Adenovirus Type 2
Irene Vazquez	Pharmacokinetics of multivesicular liposomal encapsulated cytarabine (DepoCyt™) following subcutaneous administration in dogs
Kathleen Weatherall	Comparison of two bandage splint constructs in an ex vivo mid-metacarpal equine fracture model

Faculty/Staff

Vicky Van Santen	Role of S1 N-terminal Domain Amino Acid Differences Among ArkDPI Infectious Bronchitis Virus Vaccine Subpopulations in Differential Binding to Chicken Tissues and Selection in Chickens
Rachel Knight	Bisphenol A and bisphenol S regulation of steroid hormone secretion in the rat testis
Jonathan Marable	Nanobody based immune checkpoint inhibitor for immunotherapy of canine cancers
Rebecca Nance	Methods for Isolation of RNA from Canine Osteosarcoma

Veterinary Student Platform Presentations

HPLC Method Development for Detection of Two Endocannabinoids; Anandamide (AEA) and 2-Arachidonylglycerol (2-AG) in Dog Plasma

Jeremy A. George[1], Crisanta Cruz-Espindola[1], Dawn M. Boothe[1]

[1]Department of Clinical Pharmacology, College of Veterinary Medicine, Auburn University, AL

Introduction: Endogenous cannabinoids (ECs) are important in the regulation of many physiologic systems, particularly in mammals. The two primary ECs are Anandamide (AEA) and 2-Arachidonylglycerol (2-AG). The ECs are ligands for a variety of receptors including cannabinoid receptors 1 and 2 and the vanilloid receptor 1, producing a myriad of physiologic responses. Dysfunctions of the EC system are being recognized in various states of disease. Understanding the normal state among species will increase our ability to understand pathology of diseases and identify targets through which therapeutic interventions might correct or prevent these diseases. The aim of this project was to develop a method utilizing high performance liquid chromatography with ultraviolet detection (HPLC-UV) that would accurately and precisely detect and quantitate AEA and 2-AG in the plasma of companion animals. The dog was chosen as the initial target species.

Methods: Multiple methods utilizing various mobile and stationary phases were employed, in order to accomplish HPLC-UV detection and quantification of AEA and 2-AG. Solid phase extraction followed by nitrogen drying to try stabilize and isolate AEA and 2-AG prior to HPLC-UV detection was used due to the degeneration of ECs when exposed to light and air.

Results: Samples were analyzed by reverse phase HPLC-UV with a Waters Sunfire C18 column (150mm x 4.6 i.d. x 5µm) and a mobile phase of 79% mobile phase A to 21% mobile phase B ratio: mixture of 10mM ammonium actetate in methanol (mobile phase A) and deionized water (mobile phase B). The flow rate was 1mL/min for a duration of 60min, UV detector was set at 200nm and 220nm, column temperature was 40°C, and 10µL of sample was injected. The limit of detection for both AEA and 2-AG were found to be 1000ng/mL (2877.4nM and 2643.4nM, respectively).

Conclusions: The goal of this project was accomplished and both ECs were detected in the samples that were spiked. However, the LOD was determined to be too high to be applicable for detecting endogenous levels of endocannabinoids in dogs. Previously reported ranges for AEA and 2-AG were 0.1-1nM and 50–500nM, respectively. Our LOD was calculated as 2877.4nM and 2643.4nM, respectively. Thus, our ability to utilize this method to detect ECs within patient samples is inadequate. In light of the high LOD the limit of quantitation (LOQ) was not pursued. In order to decrease our LOD to performable levels and establish an LOQ applicable to patient samples we will begin to move forward with ultra-performance liquid chromatography coupled with mass spectroscopy (UPLC-MS).

Acknowledgements: Boehringer Ingelheim Veterinary Scholars Research Program. Department of Anatomy, Physiology, and Pharmacology. Dr. Dawn Boothe, Crisanta Cruz-Espindola, and Christina Hargis for their mentorship and guidance throughout this project.

Obesity in Mice: Acute vs. Chronic Effects of High-Fat Diet Feeding

Brandon Weyhing, Han Fang, Zhuoyue Li, Henri Alexandre Giblot Ducray, Ludemila Globa, Iryna Sorokulova and Robert Judd
Department of Anatomy, Physiology and Pharmacology, College of Veterinary Medicine, Auburn University, AL

Introduction: Obesity is a growing concern throughout America due to high caloric intake and/or lack of burning sufficient calories throughout the day. C57BL6 mice are commonly used in obesity study because of their rapid weight gain in response to high-fat diet (HFD) and propensity to develop obesity-related complications similar to those observed in humans. When fed a HFD, they deposit fat throughout the body and undergo physiological changes as their bodies adapt to excess caloric consumption. The objective of this study was to compare the acute (3 week) and chronic (20 week) effects of feeding a HFD to mice in order to observe when there were significant changes in body weight, organ mass and microbial alterations within the gut.

Methods: C57BL6 Mice were fed either a chow (10% fat) or HFD (60% fat) for 3 weeks (acute) and 20 weeks (chronic). Mice were weighed every four days throughout the study. Serum and tissues were collected at the end of the study. Data was collected to compare body weights, blood glucose levels, epididymal white adipose tissue (EWAT) weight, liver weight, colon length, and microbiome composition.

Results: The HFD mice from each study displayed increases in body weight that were significantly higher than the control mice. Normalized EWAT weights were significantly higher in the 3-week study when compared to the control group and liver weights showed no significant differences. In the 20-week study, EWAT weight of the HFD mice was similar to the control group, while the liver weights were significantly increased for those fed a HFD. No changes were seen in colon length. HFD mice in the chronic study had a higher amount bifidobacterium and lower haemoltytic microbiota bacteria when compared to the chronic control group. Microbial comparisons have not been reported for the acute study yet.

Conclusions: At some point between 3 weeks and 20 weeks there is an inflection point at which ectopic fat distribution occurs. Once the EWAT maximizes its accumulation ability, fat is distributed to the liver and other organs. Further studies are being performed to identify this inflection point and better understand when the body undergoes changes in fat deposition.

Acknowledgements: Boehringer Ingelheim Summer Scholars Program

Commensal metabolites facilitates allergen-induced dendritic cell activation and inflammation

Elizabeth Manson, Anil Kumar Jaiswal[1], and Amarjit Mishra[1]

From the Laboratory of Lung Inflammation[1], Department of Pathobiology, College of Veterinary Medicine, Auburn University, Auburn, AL 36849

Background: The metabolic-sensing G-protein coupled receptors (GPCRs) such as GPR41 (FFAR3), GPR43 (FFAR2), GPR 81 (Lactate receptor; HCA1), or GPR109A (HCA2R) are widely expressed in adipocytes, intestinal epithelial cells, epidermal Langerhans cells, and peripheral blood mononuclear cells. These receptors are activated by commensal metabolites like short-chain fatty acids (SCFAs): acetate, propionate, and butyrate. Studies on knockout mice implicate that they play a significant role in chronic inflammatory disease like obesity, colitis, asthma, and arthritis. However, the expression and role of these metabolic-sensing receptors on antigen-presenting cells like dendritic cells during allergen sensitization have not been studied.

Objective: To assess whether the expression patterns of these metabolic-sensing G-protein coupled receptors by dendritic cells modulates the activation and function.

Methods: Primary bone marrow cells from mice were cultured for 7 days in presence of GMCSF (Bone marrow derived dendritic cells; BMDCs) and receptor expressions were assessed by real-time PCR (RT-PCR). Using multi-color flowcytometry technique, allergen (house-dust mite; HDM)-sensitized dendritic cells were evaluated for activation markers in presence of analogues of SCFAs.

Results: HDM-pulsed BMDCs cultured in presence of butyrate drives differentiation towards plasmacytoid phenotype, thereby suppress HDM-induced activation of DCs. Furthermore, using Gpr109a knock-out mice, we show that suppression of DC function by butyrate is independent of Gpr109a receptor.

Conclusion: This suggests a possible role for butyrate in allergen-induced DC- activation and modulating inflammation.

Acknowledgment: Boehringer Ingelheim Veterinary Scholars Program.

Localization and Quantification of Cannabinoid Receptors in Canine Tissue

Matthew E. Miller[1], Kamoltip Thungrat[1], Jey W. Koehler[2], and Dawn M. Boothe[1]
[1]Clinical Pharmacology Laboratory, College of Veterinary Medicine, Auburn, AL
[2]Department of Pathobiology, College of Veterinary Medicine, Auburn University, AL

Introduction. The endocannabinoid system (ECS) is comprised of endogenous signaling molecules known as endocannabinoids, and the G-protein-coupled receptors to which they bind. In recent decades, research has found relationships between the ECS and memory, nociception, inflammation, appetite, metabolism, and more.

In the interest of providing a framework for the eventual development of safe and effective cannabinoid therapies in veterinary species, this paper sought to characterize the two predominant cannabinoid receptors—CB1R and CB2R—by quantification and localization. While many findings from previous studies were confirmed, such as the high concentration of CB1R in gray matter and the high concentration of CB2R in blood and lymph nodes, the study also found unexpectedly high quantities of CB2R in both the male and female gonads. Additionally, unexpectedly low levels of CB2R expression were found in the lung and the liver compared to human and mouse models.

Methods. Tissue samples were acquired from living adult dogs that presented to the AU-SATH Surgery Department for procedures related to the tissues obtained. Following collection, the tissue samples were placed into either RNA*later*® or formalin. RNA*later*® samples were stored until processing. Formalin samples were submitted to histopathology for processing. In all, 35 tissue samples were collected in RNA*later*®, and 12 were collected in formalin.

RNA was extracted from tissues stored in RNA*later*®, converted to cDNA, and quantified using quantitative PCR (qPCR). The data were reported as ratios of *CB1R* or *CB2R* gene expression to the constitutively-expressed housekeeping gene *B2M*.

Immunohistochemistry was run using previously-described antibodies, and selective staining was verified by Western blot.

Results. Previously undescribed findings immunohistochemistry were limited; CB2 receptors stained most darkly in the endothelial cell membranes of most tissues, with less-significant staining scattered throughout the parenchyma, localized microscopically to the cell membranes.

Quantification showed high expression of *CB1R* gene in the blood, brain, testicles, ovary and uterus, but low expression in kidney, lung, liver and lymph node. Expression values for the *CB2R* gene were high in the lymph node and reproductive tissues, but low in the lung, liver, kidney and skin.

Conclusions. These results invite future investigation into the reproductive applications of cannabinoids, as well as possible upregulation following exogenous exposure to explain the relative low expression of *CB1R* in liver and lung tissues. Quantification of specific regions of the canine brain may also prove useful in the development of pharmaceutical cannabinoids.

Acknowledgments. The author would like to thank the histopathology lab for their assistance with immunohistochemistry, Dr. Mansour's lab for assistance with Western blotting, and the clinical pharmacology lab for their mentorship this summer.

Evaluation of semen production in boars given an IAV-S vaccine

Jonathan Tubbs[1], Seth Krantz[2], Kris Kovach[3], Seth Playter[3], Crista Goodell[4], Jeff Luebbe[4]
[1]Auburn University College of Veterinary Medicine, Auburn, Alabama; [2]Tosh Farms LLC, Henry TN; [3]Boehringer Ingelheim, Ames, IA; [4]Boehringer Ingelheim, Duluth, GA

Introduction. Influenza A virus in swine (IAV-S) is a globally endemic disease that can have significant respiratory and performance impact in infected animals. Fever from IAV-S infection is of specific concern for boars as it can detrimentally affect semen quality and production for several weeks post pyrexia. The objective of this project was to evaluate the use of an attenuated live IAV-S vaccine in boars through clinical observations and semen quality parameters. The results of this study will aid in vaccine decisions for producers with disease pressure due to IAV-S.

Methods. This study was performed at a 126 head commercial boar stud located in the southeastern U.S. from June to August 2018. Semen collection occurred once per week, with all boars collected either Sunday or Thursday evenings. The Thursday boars were selected for vaccinate group, the Sunday boars the control group. Each group contained at least 60 boars; age not balanced between collection groups. The vaccinate group was administered a single dose of an attenuated live IAV-S vaccine during the collection process. Boars were observed daily. Baseline semen data from 10 weeks preceding the study were compared to the subsequent 8 weeks following the vaccination event. Semen production parameters were assessed to determine total sperm production, morphology, and motility. Averages were calculated for time periods prior to and after vaccination.

Results. For the reported measures of total sperm production, morphology and motility, vaccinated and unvaccinated boars performed similarly as shown in Table 1.

Table 1.

	Non-Vaccinates		***Vaccinates***	
	Pre-Vaccination	Post-Vaccination	Pre-Vaccination	Post-Vaccination
Normal Morphology (%)	97.13	96.97	97.15	96.80
Total Motility (%)	87.83	86.77	88.20	86.41
Sperm Production (Billions/ejaculate)	73.31	79.72	76.55	76.81

Conclusions. Boar studs monitor key performance indicators as productivity is a way to assess health. Factors known to impact these parameters are age (increasing production), season (reducing motility and other) and diseases (highly impactful particularly with fever). In this study, boar age was not balanced, which may have contributed to differences in starting performance between groups. However thereafter, the data demonstrated the natural impact of boar maturation and season in addition to vaccination on average sperm production (modestly higher over time), and average motility (modestly lower as the summer progressed) respectively. Both groups were affected similarly. A recent publication noted the impact of IAV-S on semen production in boars affects semen quality and production by reducing total sperm production, percent motility and percent normal morphology. The results of this study indicate semen quality and production in boars vaccinated with an IAV-S vaccine remained comparable to unvaccinated cohorts.

Acknowledgments. Tosh Farms, LLC; Boehringer Ingelheim; Iowa State SVIP

Decreasing radial contact area results in a higher coefficient of friction on articular cartilage

Hannah K. Himmelmann, Reid Hanson[1], and Robert L. Jackson[2]
[1]Department of Equine Sports Medicine and Surgery
[2]Department of Mechanical Engineering

Introduction: Joints are well known for their ability to withstand high loads with minimum damage. Articular cartilage is a main element providing lubrication in joints. Multiple lubrication mechanisms are observed within joints. It is important to understand how joint friction works for disease purposes. Measuring the coefficient of friction (COF) of a sample of cartilage under specific conditions can help explain friction mechanisms in a joint. There were two hypothesis for this study: A smaller radial contact area on the articular cartilage will produce a higher COF under varying pressures and constant force, and a smaller radial contact area on the articular cartilage will produce a higher COF under varying force and varying pressure.

Methods: The study consisted of two parts; First, articular cartilage samples were collected from horses euthanized for reasons unrelated to this study. Articular cartilage was collected from the left and right distal, medial aspect of the radius. This side was cut into roughly a 4 cm^2 sample which was used for testing. Tests were run on the samples within 24 hours of cutting. The sample was mounted and a phosphate buffer saline solution filled the bowl until the articular cartilage sample was slightly submerged.
Five tests, each five minutes in length, were run on each articular cartilage sample. Each test involved a different sized steel ball. Steel balls sized 1/16 in., 1/8 in., ¼, in., ½, in., and 1 in. were used. The study used a Bruker Universal Mechanical Test (UMT) machine. A randomized number generator was used to determine the order the tests were run. The normal load and tangential load data was recorded by the UMT software where it was then extracted and graphed. An ANOVA was used to calculate the results.
Part one of the study used a consistent 5 N of force for each sized steel ball. Part two of the study changed the force along with the size steel ball that would result in the same pressure. See chart for forces.

Diameter of Steel Ball (in)	Force (N)
1/16	1.99
1/8	3.15
¼	5
½	7.94
1	12.61

Results: Part one results: The COF of the $1/16^{th}$ inch ball was significantly higher than the others. Part two results: The COF of the $1/16^{th}$ inch ball was significantly higher than all others, the $1/8^{th}$ inch ball COF was significantly higher than ½ and 1 inch ball COF, but not the ¼th inch ball COF. The ¼th, ½, and 1 inch ball COFs were not significantly different from each other.

Conclusion: When applying the same amount of force, the smaller surface area will produce a larger COF. When maintaining the same contact pressure on the cartilage by applying different forces, the smaller surface area will still produce a larger COF. Contact pressure on the articular cartilage did not significantly contribute to COF. Therefore, we can conclude that smaller radius of curvatures result in higher COFs in articular cartilage contacts.

Acknowledgments: Thank you to Cole Baker and everyone in necropsy and the Boehringer Ingelheim Veterinary scholarship program for funding.

Graduate Student Platform Presentations

Normal Electrocardiogram of Conscious Bald Eagles (*Haliaeetus Leucocephalus*)

Sara Collins, D.V.M [1], SeungWoo Jung, D.V.M., Ph.D., Dipl. D.A.C.V.I.M. [1], and Seth Oster, D.V.M [1,2]
[1] Department of Clinical Sciences, College of Veterinary Medicine, Auburn University, 1220 Wire Road, Auburn, AL 36849, USA
[1,2] Southeastern Raptor Center, Auburn University, 1350 Pratt-Carden Dr., Auburn, AL 36849, USA (Oster)

The goal of this study was to identify normal electrocardiographic (ECG) patterns and to establish reference ranges of normal ECG parameters in conscious bald eagles (*Haliaeetus leucocephalus*). ECG was performed in 9 healthy, conscious eagles. The standard bipolar and augmented unipolar limb leads were used to analyze morphologic patterns of P-QRS-T waveforms. The waveforms recorded at the standard calibration (50 mm/sec, 10 mm=1 mV) were analyzed to determine parameters of PR interval, PR segment, QRS duration, ST segment, QT interval, and amplitudes of P, QRS, and T waves. Rhythm, heart rate (HR), mean electrical axis (MEA), and occurrence of ST slurring were also characterized. The MEA for the frontal plane was calculated using leads I and aVF. Normal sinus rhythm was documented from all subjects. The median heart rate was 273 beats/min (bpm) (range: 214 ~ 429 bpm). The mean heart rate was 290 ± 59 beats/min (bpm). P waves were predominately positive in standard bipolar lead II. In leads I, II, III, and aVF, the dominant pattern of the QRS complexes was rS, whereas in leads aVR and aVL the pattern was always qR. T waves were predominately positive in lead II. The median MEA was -110° (range: -123° ~ -100°) and the mean MEA was -110° ± -6.6°. This study provides the first electrocardiographic reference data in conscious bald eagles, which will improve the recognition and diagnosis of electrophysiologic abnormalities in both captive and wild birds. It also evaluates the practicality and value of acquiring ECGs on conscious bald eagles by comparing the ECG values previously reported in anesthetized bald eagles.

Characterization and functional analysis of the putative calcium-binding protein, ankef1

Jeff Daniel and Jennifer Panizzi
[1]Department of Anatomy, Physiology, and Pharmacology, College of Veterinary Medicine, Auburn University, AL

Introduction. This project's long-term goal is to define the expression patterns and developmental function(s) of ankyrin and EF-hand containing protein 1 (ankef1, ankrd5, or anr5). In our lab, Ankef1 was isolated from a yeast two-hybrid (Y2H) screen as a potential interactor with ccdc103, a dynein attachment factor that is localized to motile cilia. While little is known about Ankef1 function, it is expressed in multiple human tissues, with strongest expression in the testis. Two ankef1 homologs are predicted to exist in the zebrafish due to genome duplication, and our lab has confirmed the presence of both homologs in zebrafish embryos. A study on *Xenopus laevis* indicated that ANKEF1 plays a role in protocadherin-mediated cell protrusion and adhesion. Interestingly, recent next-generation sequencing (NGS) and genome-wide association studies (GWAS) studies in humans showed an association of ANKEF1 polymorphisms or abnormal levels of ANKEF1 transcripts with prostate cancer risk, schizophrenia, glioblastoma, thoracic aortic aneurysms and dissections, pediatric acute lymphoblastic leukemia, and nasopharyngeal carcinoma. Hypothesis: Ankef1 is required for proper development and function of ciliated tissues.

Methods. Our lab uses a combination of developmental, genetic, and biochemical methods in the zebrafish to model ANKEF1 function in vertebrate development. Our research has clarified expression patterns of ANKEF1 and has begun to address the gap in knowledge about the functional role of the gene in vertebrates. Methods used: PCR, molecular cloning, CRISPR/Cas9, morpholino oligonucleotides, microinjection, light microscopy, whole-mount in situ hybridization (WISH).

Results. Whole exome sequence data from our work on another project was searched for both ANKEF1A/B transcripts and were present in 2 dpf embryos. Coding regions for both ANKEF1A and ANKEF1B have been amplified from embryonic (AB line, mix of 13 stages) cDNA and inserted into plasmid vectors. We have used established protocols for WISH to observe tissue expression of ANKEF1A/B during selected stages of development. WISH showed ubiquitous expression during early stages, with specific staining in the dorsal midline and DFCs, as well as later stages in the otic vesicle, swim bladder, and pharyngeal region. Our lab has demonstrated CRISPR/Cas9 proof-of-concept KO of slc45a (albino phenotype; positive control) and ccdc103 (immotile cilium positive control). Sanger sequencing confirmed that we have also knocked out ANKEF1A with the CRISPR/Cas9 system, revealing a shortened phenotype similar to morpholino knockdown in *Xenopus*. We have also used CRISPR/Cas9 to introduce ANKEF1A germline mutations have confirmed heterozygous ankef1a mutations in the F2 generation.

Conclusions. Ubiquitous expression of both ANKEF1A/B transcripts revealed by WISH and RT-PCR suggests a functional role in all stages of zebrafish development. Furthermore, specific staining to the otic vesicle and DFCs suggest a possible role in tissues with motile cilia. Splice-blocking MO knockdown on ANKEF1A in our lab has shown that heart loop laterality—a process mediated by motile cilia—is disrupted either by reduced zygote-derived normal transcripts or interference from ankef1a proteins translated from the abnormally spliced mRNA.

Acknowledgments. Expert guidance was provided by Dr. Jennifer Panizzi. This work was made possible by funding from the College of Veterinary Medicine AHDR grant and the Department of Anatomy, Physiology, and Pharmacology.

Intravenous delivery of AAV gene therapy in GM1 gangliosidosis

Amanda L. Gross[1,2], Heather Gray-Edwards[3], Ana Rita Batista[4,5], Stacy Maitland[4,5], Miguel Sena-Esteves[4,5], Douglas R. Martin[1,2]

[1]Scott-Ritchey Research Center, Auburn University College of Veterinary Medicine, Auburn, AL
[2]Department of Anatomy, Physiology, & Pharmacology, College of Veterinary Medicine, Auburn University, AL

[3]Department of Radiology, University of Massachusetts Medical School, Worcester, MA

[4]Department of Neurology, University of Massachusetts Medical School, Worcester, MA

[5]Horae Gene Therapy Center, University of Massachusetts Medical School, Worcester, MA

Introduction. GM1 gangliosidosis is a hereditary lysosomal storage disease caused by a deficiency of lysosomal β-galactosidase (β-gal). The most common form of GM1 gangliosidosis affects children, is fatal by 4 years of age, and is characterized by rapidly progressing neurological disease. Outside of palliative and supportive care, there is no effective treatment for GM1. Adeno-associated viral (AAV) therapy has proven effective in a well-characterized feline model of GM1 gangliosidosis, demonstrating a greater than 10-fold increase in lifespan after injection to the brain thalami and deep cerebellar nuclei. Intravenous delivery was tested to circumvent the surgical risk of the intracranial approach while potentially increasing cortical and systemic biodistribution

Methods. AAV9 containing feline B-gal was delivered at a total dose of 1.5e13 vector genomes/kg body weight at approximately 1 month of age. The six animals included in the study were divided into two cohorts: 1) a long term group, which was followed to humane endpoint, and 2) a short-term cohort, with samples collected 16-week post treatment. Animals were assessed using a clinical rating score to determine disease progression. After the designated time point, biodistribution of β-gal was assessed using a synthetic enzyme substrate. Brain architecture and metabolites were analyzed using magnetic resonance imaging (MRI) and spectroscopy (MRS), respectively.

Results. The long-term group had an average 5.3-fold increase in life expectancy, with both animals showing limited neurological signs. In both cohorts, there was an increase in the distribution and activity of β-gal, reaching normal levels in the cerebellum, spinal cord (cervical, mid-thoracic and lumbar regions), and select peripheral tissues. Magnetic resonance imaging showed a normalization of the brain architecture post treatment. Magnetic resonance spectroscopy showed normalization of the metabolites glycerophosphocholine and phosphocholine which suggests reduced demyelination.

Conclusions. Restoration of β-gal to levels just 0.1 fold normal has shown therapeutic effect, and with IV gene therapy there is an even greater restoration of β-gal activity. Additionally, normalization of brain architecture and metabolites indicate amelioration of cell damage and demyelination. Taken together, this data strongly supports the use of IV injection of AAV gene therapy as a safe and effective treatment for GM1 gangliosidosis.

Acknowledgments. This research was funded by Porter's Fund, private donations, and the Scott-Ritchey Research Center

I*n Vitro* and *Ex Vivo* Cyclo-oxygenase Inhibition by Flunixin Meglumine and Firocoxib in the Asian Elephant (*Elephas maximus*)

Jack J. Kottwitz[1] and Dawn M. Boothe[1]
[1]Department of Anatomy, Physiology, and Pharmacology, Auburn University, AL

Introduction. Nonsteroidal anti-inflammatory drugs (NSAIDS) are the most commonly administered class of drugs for pain and discomfort in captive elephants. NSAIDs exert their effects by inhibiting cyclo-oxygenase (COX) isoenzyme activity which in turn limits prostanoid production, subsequently decreasing inflammation and associated pain. In mammals, two main COX isoforms have been identified: COX-1 which is the constitutive form that plays an important role in the regulation of tissue blood flow and is the main source of prostaglandins for gastric epithelial cytoprotection, and COX-2 which is predominately expressed during inflammation. While NSAIDs are effective at reducing inflammation and associated pain, they also can have severe adverse effects, including gastric ulceration and kidney damage.

Methods. The prostanoids thromboxane-B2 and prostaglandin-E2 with associated prostaglandin-E2 metabolites were utilized as indicators of COX-1 and COX-2 isoenzyme activity. An *in vitro* coagulation-induced thromboxane-B2 assay was used to determine drug concentration COX-1 inhibition curves in clotted Asian elephant blood. An *in vitro* lipopolysaccharide induced prostaglandin-E2 and metabolite assay was utilized to determine COX-2 inhibition curves in whole blood. Adult Asian elephants (1 male and 2 females) were administered flunixin meglumine at a dose of 1.1 mg/kg PO q 24 hours x 3 doses or firocoxib (2 males and 4 females) at a dose of 0.1 mg.kg PO q 24 hours x 8 doses. The above assays were then utilized to determine *ex vivo* thromboxane B2 and prostaglandin E2 + metabolite levels as an indication of COX-1 and COX-2 isoenzyme activity in Asian elephants prior to drug administration and with each of these drugs administered sufficient times to reach serum steady state. *Ex vivo* concentrations of thromboxane-B2 and prostaglandin-E2 + metabolites were also determined in Asian elephants receiving long term (> 3 months) administration of firocoxib to manage painful conditions such as osteoarthritis.

Results. Flunixin meglumine demonstrated inhibition of both COX-1 and COX-2 isoenzymes, with preferential inhibition of COX-1 *in vitro*. Firocoxib demonstrated virtually exclusive inhibition of COX-2 *in vitro,* with minimal inhibition of Cox-1 detected. Flunixin meglumine induced more than a 10 fold decrease in COX-1 activity *ex vivo* after multiple doses sufficient to reach serum steady state, with little change in COX-2 activity from baseline levels. Firocoxib demonstrated little change in serum COX-1 activity *ex vivo* after sufficient doses to reach serum steady state and after long term administration. A paradoxical increase in COX-2 isoenzyme activity was noted *ex vivo* after sufficient doses were administered to reach serum steady state, but these levels subsequently decreased with long term administration.

Conclusions. Compared to flunixin meglumine, firocoxib has COX-1-sparing effects *ex vivo* in Asian Elephants. The substantial reduction in COX-1 activity caused by flunixin meglumine may indicate an increased risk for negative side effects.

Acknowledgments. Thank you to the Morris Animal Foundation for financial support of this study. Thank you to Dr. Judd and his lab for analytical assistance. Thank you to Crisanta, Cristina, Benji, and Roy of the Clinical Pharmacology Laboratory for laboratory support

Current Image Analysis Techniques to Quantify Adipocyte Area

Anne S. Maguire[1,2], Lauren N. Woodie[3], Douglas R. Martin[1,2], Robert L. Judd[1], Emily C. Graff[4], Michael W. Greene[3]
[1]Department of Anatomy, Physiology, & Pharmacology, College of Veterinary Medicine, Auburn University, AL
[2]Scott-Ritchey Research Center, College of Veterinary Medicine, Auburn University, AL
[3]Department of Nutrition, Auburn University, AL
[4]Department of Pathobiology, College of Veterinary Medicine, Auburn University, AL

Introduction. Obesity is a prevalent pathologic condition in humans and companion animals in which adipose tissue plasticity plays a significant role. Adipocytes are the primary cells of adipose tissue that accommodate extra energy through hypertrophy (expansion of individual cells), or hyperplasia (creation of more cells). Therefore, accurate quantification methods of adipocyte area are crucial to the investigation of novel therapeutic interventions for obesity. Current methods primarily consist of image acquisition through digital cameras fitted to microscopes followed by the manual outlining of cells in software that calculates individual adipocyte areas. Disadvantages of these methods include small sample size, bias in obtaining and annotating images, and high time and labor costs. The recent advent of digital slide scanners, whole slide image analysis, and open-source software shows promise for resolving these issues. To assess the applicability of current image acquisition and analysis methods to the calculation of adipocyte areas, we compare a traditional method of adipocyte area quantification (microscope camera with ImageJ software), with two modern whole-slide analysis methods: a proprietary software (Visiopharm), and a combination of two open-source programs (QuPath and ImageJ).

Methods. Epididymal adipose tissue was collected from two groups of mice fed standard chow or high fat diet (HFD). Slides were stained with hematoxylin and eosin, then analyzed with the following methods:

1) Microscope camera + ImageJ: The area of each adipocyte in one photomicrograph was calculated using a publicly available plugin.
2) Slide scanner + QuPath + ImageJ: Slides were digitally scanned with an Aperio ScanScope at 40x, then analyzed using an algorithm we developed in QuPath and ImageJ to quantify the area of each adipocyte in the entire slide.
3) Slide scanner + Visiopharm: Slides were scanned as in Method 1, then a Visiopharm algorithm we developed calculated the area of each adipocyte across the entire slide.

Results. The average number of adipocytes counted varied widely between each method, but the areas of recognized cells were quantified consistently. Method 1 counted significantly fewer cells than the whole-slide analysis methods 2 and 3 (94.1% and 96.2%, respectively). This small sample size led to high variability in areas measured by method 1 (R^2 for 1 vs 2: 0.71, R^2 for 1 vs 3: 0.66), especially in the HFD group. Though method 2 counted 36.3% fewer cells than method 3, this decrease in power did not negatively affect the variance of measured areas (R^2 for 2 vs 3: 0.94). Though an initial increase in complexity was required to develop the algorithms for methods 2 and 3, all methods involved similar amounts of time and labor for routine analysis.

Conclusions. Newer methods of whole slide analysis provide a significant sample-size advantage over more traditional methods. The open-source programs QuPath and ImageJ used in combination provide an adequate sample size and ease of use that negate the necessity for the high-cost proprietary software Visiopharm.

Acknowledgements. Cynthia Tiley Hutchinson for technical assistance

Angiotensin II, the innate immune system, and blood-brain barrier disruption in neurogenic hypertension

Francesca E. Mowry, Sarah C. Peaden, and Vinicia C. Biancardi

Department of Anatomy, Physiology, and Pharmacology, College of Veterinary Medicine, Auburn University, AL, United States

Introduction. Neurogenic hypertension is associated with dysregulation of the renin-angiotensin systems, increased sympathetic nervous system (SNS) activity, and chronic low-grade inflammation. Our previous work points to angiotensin II (AngII) as a driving force behind blood-brain barrier (BBB) disruption in hypertension, and as a mediator of Toll-like receptor 4 (TLR4) stimulation through AngII type 1 receptors (AT1R) in hypothalamic microglia (Biancardi, 2014 [*Hypertension*]; Biancardi, 2016 [*Am J Physiol*]). We propose that abnormal activation of microglial TLR4 by AngII via AT1R cross-talk within key cardioregulatory nuclei creates a feedforward pro-hypertensive loop with BBB disruption, neuroinflammation, and sympathoexcitation in the context of neurogenic hypertension.

Methods. 8-week-old spontaneously hypertensive rats (SHR) were treated by oral gavage with an AT1r antagonist, Losartan (SHRLos; 20mg/kg/day; 4 weeks), and age-matched with sham SHRs and normotensive Wistar Kyoto (WKY) rats. Mean arterial pressure (MAP) was measured weekly via indirect tail-cuff with a volume-pressure system. Immunofluorescence assays with primary antibodies against TLR4 and IBA1 were performed in the paraventricular nucleus of the hypothalamus (PVN) and rostral ventrolateral medulla (RVLM) to determine TLR4 protein density and microglial activation status. A second SHR cohort was treated with TAK-242, a TLR4 inhibitor (2mg/kg/day; *i.p.*; 14 days), and paired with SHR and WKY controls. Indirect tail-cuff MAP was measured on alternating days. Extravasation of a low molecular weight dextran-conjugated dye in the PVN and RVLM was used as an assessment of BBB integrity. Direct MAP was recorded in conscious rats and SNS activity was determined by ganglionic blockade with hexamethonium bromide (20mg/kg; *i.v.*).

Results. 4-week blockade of AT1R normalized MAP in Losartan-treated SHR. Compared to WKY, TLR4 density in the PVN and RVLM of SHR was increased by 104% and 113%, respectively, while SHRLos values were normalized. Microglial skeletal analysis showed significantly elevated levels of microglial activation in hypertensive SHR versus normotensive WKY, which was abrogated with Losartan treatment. 14 days of treatment with a TLR4 antagonist significantly reduced MAP compared to control SHR. BBB permeability analysis showed complete abolishment of the leakage observed in the PVN and RVLM of untreated SHRs. TLR4 inhibition also normalized SNS activity, which was significantly elevated in SHRs compared to WKYs.

Conclusions. Our findings provide strong support for AngII-induced AT1R-TLR4 interactions in the pathophysiology of neurogenic hypertension, specifically in mediating BBB disruption, aberrant microglial activation, and sympathoexcitation.

Acknowledgments. This work was funded by the AHA14SDG20400015 to VCB.

Development of Oncolytic Adenovirus Library Displaying Synthetic Nanobodies in Place of Fiber Knob

Damien Ruiz[1], Natalie Heape[2], Jonathan Marable[1], Maninder Sandey[1]

[2]Department of Pathobiology, College of Veterinary Medicine, Auburn University, AL
[1]College of Veterinary Medicine, Auburn University, AL

To date, adenovirus (Ad) is one of the most extensively utilized viral vectors for gene therapy applications. In the context of cancer treatment options, oncolytic virotherapy presents a powerful and exciting strategy for cancers that are resistant to currently available therapies. Oncolytic adenoviruses (Ad) are anticancer agents specifically designed to selectively infect and kill malignant cells without harming the normal tissues. As an added benefit, direct tumor cytolysis primes an immune response against tumors due to the production of cytokines and release of tumor antigens. However, the realization of the full therapeutic potential of oncolytic adenoviruses as therapeutic agents for cancer has been hindered by its broad native tropism. Adenovirus entry into the cells is a two-step process, mediated by the interaction of its fiber knob with the coxsackie adenovirus receptor (CAR) followed by interaction between the arginine-glycine-aspartic acid (RGD) sequence of the penton base and αv integrins. However, the lack of cell-specificity of infection due to the widespread distribution of native adenovirus receptors often mitigates the pharmacological goal of tumor-specific virus infection and oncolysis. Moreover, several studies have also shown that the cancer cells express CAR receptor at very low levels. Numerous strategies, including the use of molecular adapter proteins and genetic modification of adenoviral capsid proteins (hexon, pIX and fiber), have been employed to alter the native Ad tropism. However, the essential requirement for these strategies to be successful is a well-characterized tumor-specific antigen. Adenovirus libraries displaying random peptides in the capsid proteins can partially overcome this problem. However, incorporation of random peptides to the adenoviral capsid proteins only provides tropism expansion rather than simple re-targeting to a specific tumor antigen*. In this proposal, we will explore the possibility of displaying a camelid nanobody library on the adenoviral fiber knob, and investigate its potential for direct selection of retargeted adenovirus against canine oral melanoma cells. Our central hypothesis for this proposal is that an adenoviral display platform expressing camelid nanobody repertoires on the fiber knob will help us to identify tumor-selective oncolytic adenoviruses. The retargeted adenoviruses will use the tumor-specific antigens to selectively infect and induce cytotoxic cell death in tumor cells without harming normal tissues.* To achieve these goals, we will construct a chimeric fiber composed of DNA sequences encoding the: 1) N-terminus of CAV2 fiber, 2) the fibritin protein of T4 bacteriophage, and 3) camelid IgG2a hinge region as a peptide linker. This chimeric fiber will be used to display diverse nanobodies amplified from a synthetic camelid nanobody library. As proof of concept, we have engineered a chimeric CAV2 fiber-fibritin molecule displaying anti-PDL1 nanobody on its surface. The fiber-fibritin chimera was synthesized, amplified by PCR and inserted it into the genome of ICOCAV15 (canine adenovirus serotype-2) using homologous recombination in yeast. Sequence analysis of the recombinant plasmids confirmed the targeted modification of the CAV2 fiber. We also constructed a stable cell line (DKcre-hPDL1) constitutively expressing human PD-L1 to propagate and amplify the ICOCAV15 displaying chimeric fiber. In future studies, we will characterize the recombinant adenoviruses including the incorporation of VHH-fiber-fibritin fusion protein into the virus, virus stability and ability to selectively infect and kill tumor cells.

Acknowledgment: Dr. Payal Agarwal, Dr. Bruce F. Smith, Dr. Ramon Alemany, Cynthia Hutchinson, Abdul Mohin Sajib.

Comparison of the cytokine and cellular profile of autologous protein solution, autologous conditioned serum, and serum incubated for 24 hours in healthy horses

Ana Velloso Alvarez[1], Anne A. Wooldridge[1], Fred Caldwell[1], and Lindsey Boone[1]

[1] Department of Clinical Sciences, Auburn University, AL

Introduction: Clinical use of autologous blood-derived intra-articular therapies such as autologous conditioned serum (ACS) or autologous protein solution (APS) has increased in horses. These products contain high concentrations of anti-inflammatory cytokines and growth factors meant to slow the catabolic degradation of articular cartilage in osteoarthritis (OA). Few studies have investigated the cytokine and growth factor composition of these products in equine blood or within horse, leaving equine practitioners little guidance for their clinical use. The objective of this study was to measure the cellular composition and concentration of important OA modifying cytokines and growth factors in equine serum, ACS, and APS.

Methods: Blood was obtained from 6 systemically healthy, adult horses. A complete blood count (CBC) was obtained from each horse immediately prior to blood collection. Blood was obtained and processed for each commercial product according to the manufacturer's instructions producing ACS and APS. ACS and APS were analyzed for white blood cell (WBC), red blood cell (RBC), and platelet (PLT) concentration. Additional blood was collected into plain glass vacutainers, incubated at 37°C for 24 hours, and then centrifuged to collect serum. Aliquots of all products (serum, ACS, and APS) were snap frozen and stored at -80°C until ELISA analysis. ELISA analysis was performed using commercially available kits for growth factor (TGF-β), anti-inflammatory (IL-1rap, and sTNF-R1), and pro-inflammatory (IL-1β, TNF-α, and MMP-3) cytokines.
Data was analyzed using a repeated measures one-way ANOVA and Tukey's post hoc analysis was performed. Significance was set at $p<0.05$.

Results: The WBC concentration of APS was increased compared to baseline blood ($p=0.0002$) and ACS ($p<0.0001$). The WBC concentration of ACS was decreased compared to baseline blood values ($p=0.0002$). The PLT concentration of APS was increased compared to baseline blood ($p=0.0309$) and ACS ($p<0.0001$). The PLT concentration of ACS was decreased compared to baseline blood ($p=0.0012$). The RBC concentration was increased in baseline blood compared to ACS ($p<0.0001$) and APS ($p=0.0002$). The concentrations of IL-1β, IL-1Ra, TNFα, IL-1β: IL-1Ra ratio, TNFα:sTNF-R1 ratio, and MMP3 were not different between incubated serum, ACS, and APS. However, sTNF-R1 was increased in incubated serum compared to APS ($p=0.0289$). The concentration of TGF-β was decreased in APS compared to ACS and incubated serum ($p=0.0047$ and $p=0.0001$ respectively).

Conclusions: Despite the varied cellular composition of ACS and APS, there are few differences in cytokine concentrations despite processing methods. More importantly, whole blood incubation with processing of plain serum produces similar, if not better cytokine and growth factor profiles compared to the commercial products. Further investigation into the use of incubated serum for treatment of joint-related injury in horses is warranted.

Acknowledgments. Project funding provided by the Birmingham Racing Committee and the Auburn University Department of Clinical Sciences. We would like to thank Qiao Zhong for technical assistance for completion of the project.

Age of Vaccination Influences Infectious Bronchitis Virus Cross-Protection

Ramon A. Zegpi, Steve Gulley, Amarjit Mishra, Vicky van Santen, Haroldo Toro

Department of Pathobiology, College of Veterinary Medicine, Auburn University, AL

Introduction.
Infectious Bronchitis virus (IBV) causes enormous economic losses to the poultry industry. Antigenically novel IBV strains continue to emerge causing disease in vaccinated chickens. Previous studies have indicated that vaccination at an early age (i.e. 1-day-old), generates suboptimal homologous protection. We hypothesized that postponing vaccination beyond day 1 of age also increases heterologous protective immunity.

Methods.
Chickens were vaccinated with a Massachusetts (Mass)-type commercially available vaccine at hatch or on days 10 or 14 after hatch and challenged with an Arkansas (Ark)–type virulent strain. After challenge, viral load in tears (qRT-PCR) and tracheal histological lesions were compared between groups vaccinated at different ages. Serum antibody levels were measured post vaccination by ELISA. The avidity of antibodies was estimated using a modified ELISA in which a chaotropic agent (GuHCl) was added to disrupt antibody-antigen interactions. Lymphocyte populations were characterized by flow cytometry.

Results.
The analysis of tracheal histopathology, and viral load demonstrated improved cross protection when vaccination is postponed. The results of both trials indicate that vaccination at a later age is associated with lower viral loads after challenge. Challenged chickens that were vaccinated on day 1 showed increased ($P<0.05$) tracheal mucosal thickness, lymphocyte infiltration, and deciliation compared to chickens vaccinated on day 10. Antibodies to Ark-type spike protein showed increased avidity in chickens vaccinated at day 14 versus chickens vaccinated on 1 of age. Harderian gland derived B and T cells are present in higher numbers in chickens vaccinated at day 1.

Conclusions.
The current findings suggest that postponing vaccination against IBV beyond day of hatch improves heterologous protection. The fact that vaccination beyond day hatch increases antibody avidity may assist explaining the enhanced cross-protection observed.

Acknowledgments.
Thanks to Allison Bird for flow cytometry analysis and Cassandra Breedlove-Kitchens for her assistance. This research was funded by USDA NIFA #2015-06934.

Faculty Platform Presentations

Effect of 3% chloroprocaine on onset of analgesia after application of high regional nerve blocks on naturally lame horses

Lindsey Boone[1], John Schumacher[1], Fred DeGraves[2], and Robert Cole[1]

[1]Department of Clinical Sciences, College of Veterinary Medicine, Auburn University, AL
[2]Department of Agriculture, Western Kentucky University, KY

Introduction. High regional nerve blocks may require 20 minutes or more before sufficient desensitization for interpretation of the block in reduction of lameness in horses. A local anesthetic that can produce a more rapid onset of analgesia would reduce down time of practitioners performing complicated lameness evaluations. Chloroprocaine is the fastest-acting local anesthetic used in people, but has yet to be tested in horses. The objective of this study was to determine if 3% chloroprocaine would significantly decrease the time to onset of analgesia when performing median and ulnar nerve blocks in naturally lame horses compared to 2% mepivacaine hydrochloride (mepHCl).

Methods. Median and ulnar nerve blocks were performed in an experimental crossover design on the naturally lame limb of six horses during two separate study periods, with a minimum washout period of three days between study periods. Nerve blocks were performed by administering 2% mepHCl or 3% chloroprocaine. Lameness was evaluated objectively using a wireless, inertial, sensor-based, motion analysis system (Lameness Locator®) prior to the high regional nerve block and every 5 minutes following administration of the nerve block for at 60 minutes and then every 15 minutes up to 120 minutes after the block was performed.

Results. The VS of vertical head movement was significantly decreased for 3% chloroprocaine compared to 2% MepHCl nerve blocks, when lameness evaluations from 5-60 min were modeled simultaneously ($P = 0.0043$). The VS of vertical head movement significantly decreased over time, when all lameness evaluations from 5-60 min were modeled simultaneously ($P < 0.0001$). Nerve blocks performed with chloroprocaine induced a significantly deeper plane of local anesthesia at 20 ($P = 0.0003$), 25 ($P = 0.0159$), 30 ($P = 0.0045$), and 40 ($P = 0.0113$) min after injection compared to nerve blocks with MepHCl. In summary, median and ulnar nerve blocks performed with 3% chloroprocaine ameliorated naturally occurring lameness more profoundly from 20-40 min than did median and ulnar nerve blocks performed with 2 % MepHCl.

Conclusions. Resolution of lameness occurred more rapidly and more profoundly for horses administered median and ulnar nerve blocks with 3% chloroprocaine compared to 2% mepHCl up to 40 mins after administration of the nerve block.

Acknowledgments. We would like to thank Jessica Brown for assistance with horse handling during the course of the study.

Sodium bicarbonate speeds and potentiates anesthesia of median and ulnar nerve blocks performed with mepivacaine

Lindsey Boone[1], John Schumacher[1], Fred DeGraves[2], and Robert Cole[1]

[1]Department of Clinical Sciences, College of Veterinary Medicine, Auburn University, AL
[2]Department of Agriculture, Western Kentucky University, KY

Introduction. High regional nerve blocks may require 20 minutes or more before sufficient desensitization for interpretation of the block in reduction of lameness in horses. A practical method to speed the onset of analgesia of these high regional nerve blocks would reduce down time of practitioners performing complicated lameness evaluations. The objective of this study was to determine if buffering mepivacaine HCl (mepHCl) with sodium bicarbonate ($NaHCO_3$) would significantly decrease the time to onset of analgesia when performing median and ulnar nerve blocks in naturally lame horses.

Methods. Median and ulnar nerve blocks were performed in an experimental crossover design on the naturally lame limb of nine horses during two separate study periods, with a minimum washout period of three days between study periods. Nerve blocks were performed by administering mepHCl alone or mepHCl mixed with $NaHCO_3$ (9 parts 2% mepHCl to one part 8.4% $NaHCO_3$). Lameness was evaluated objectively using a wireless, inertial, sensor-based, motion analysis system (Lameness Locator®) prior to the high regional nerve block and every 5 minutes following administration of the nerve block for at 75 minutes.

Results. The vector sum of vertical head movement was significantly decreased for buffered mepHCl compared to unbuffered mepHCl ($P = 0.0111$). Buffered mepHCl ameliorated lameness more rapidly than did unbuffered mepHCl when performing median and ulnar nerve blocks (10 vs 20 minutes with a 70% reduction of the initial VS; 20 vs 35 minutes, assuming lameness was resolved when VS ≤ 8.5 mm). Nerve blocks performed with buffered mepHCl induced a significantly deeper plane of local anesthesia from 10-40 minutes after injection compared to nerve blocks with unbuffered mepHCl alone.

Conclusions. Resolution of lameness occurred more rapidly and more profoundly for horses administered median and ulnar nerve blocks with buffered mepHCl compared to unbuffered mepHCl. Practitioner wait time for onset of analgesia for high regional nerve blocks can be cut in half when mepHCl is buffered with $NaHCO_3$.

Acknowledgments. We would like to thank Jessica Brown for assistance with horse handling during the course of the study.

A Comparison of General Anesthesia with Sedation and Local Anesthesia for Castration of Dogs: a Preliminary Study

Erika Silva Cuzmar[1], John Schumacher[2], Thomas Passler[2], William R. Ravis[3]

[1]Encargada Área de Cirugía, Instituto de Ciencias Clinicas Veterinarias, Universidad Austral de Chile, Valdivia, Chile
[2]Department Clinical Sciences, College of Veterinary Medicine, Auburn University, AL
[3]Department of Drug Discovery and Development, Auburn University, AL

Introduction. Male dogs are routinely castrated for population control and to decrease their impulse to roam. In many developing countries, free-roaming dogs transmit zoonotic diseases, most importantly rabies. Roaming dogs are likely to suffer from malnutrition, starvation, fight wounds, abuse, and sexually-transmitted diseases. Low-cost neuter programs significantly promote spay/neuter procedures. If dogs could be castrated using only sedation and local anesthesia for restraint and analgesia, complications and expense associated with general anesthesia could be avoided. Because men and horses are routinely castrated painlessly using only sedation and local anesthesia, we hypothesized that dogs could be similarly castrated.

Methods. Twenty-four dogs in the local anesthesia treatment (LA) were castrated while sedated with xylazine and after injecting each testis and the site of incision with lidocaine, and 24 dogs in the general anesthesia treatment (GA) were castrated while anesthetized with xylazine and propofol. All dogs were sedated with xylazine (1mg/kg, IM). Dogs in GA treatment were administered propofol (4.4mg/kg, IV) as a bolus once they became sedated and were re-administered propofol (2.2 mg/kg, IV) if signs of insufficient anesthetic depth were evident during surgery. Dogs in the LA treatment were administered 2% lidocaine subcutaneously in the pre-scrotal area and intratesticularly until a slight swelling of the testis could be felt. Doses of lidocaine ranged from 4.2 mg/kg to 14.9 mg/kg (mean 10.7 mg/kg ± 2.4 mg/kg). Movement scores and heart and respiratory rates (HR, RR) were determined before sedation, 3 minutes after sedation and immediately prior to the skin incision. Baseline data were collected immediately before the skin incision.

Results. One dog reacted painfully to intra-testicular injection of lidocaine. Nine dogs in the LA treatment and 16 dogs in the GA treatment did not move during castration. Movement of dogs in the LA treatment did not interfere with surgery and subjectively appeared to be random rather than associated with pain perception. The average percentage change in HR from baseline values was not significantly different between treatments. During surgery, the percentage decrease in RR from baseline was significantly greater in the LA subjects than subjects that were in the GA treatment. Based on objective assessments, indicators of pain were not different in LA- treated dogs from in dogs in the GA treatment.

Conclusions. Other than observing a painful response of one dog to intratesticular injection of lidocaine, no problems were encountered using sedation and local anesthesia to castrate 24 dogs. These results suggest that the combination of IM xylazine and local anesthesia of the surgical site provides a practical option for castration of dogs. Given these findings, this protocol warrants further study for castration of dogs when general anesthesia is inappropriate.

Acknowledgments. The study was funded by Universidad Austral de Chile, Valdivia, Chile.

Undergraduate Student Poster Presentations

Identification of Circulatory microRNA in Canine Cancer Patient Liquid Biopsies

Hannah C. Harris[1], Will P. Kretzschmar[1], Taylor D. Flaat[3], Payal Agarwal[2], Bruce F. Smith[2,3]
[1] College of Sciences and Mathematics, Auburn University, AL
[2] Department of Pathobiology, College of Veterinary Medicine, Auburn University, AL
[3] Scott-Ritchey Research Center, College of Veterinary Medicine, Auburn University, Al

Introduction. Early detection of cancer is often the key to increasing patient survival. At this point, many diagnostic techniques do not detect cancer early enough for optimized treatment. Circulating exosomal microRNAs (miRNA) can provide an easier, less invasive diagnostic tool for virtually all cancer types. In a previous study, several miRNAs were identified to be broadly upregulated in cultured canine tumors and tumor lines through deep gene sequencing. However, these miRNAs were not detected in live patient blood samples using Quantitative Reverse Transcriptase PCR (Q-RT-PCR). The purpose of this study is to validate these miRNA Q-RT-PCR assays in cell culture and compare results to that of the deep gene sequence.

Methods. 13 cell lines and 3 primary cells were grown in exosome free media in cell culture. Exosomal RNA was isolated from each cell type, and used to synthesize cDNA for qPCR. Micro RNA 16 (miR16) was used as a control qPCR to confirm the presence of cDNA. Q-RT-PCR of the experimental samples is pending. miR16 will be used both as a positive reaction control and as a normalizing reference for the experimental miRNAs

Results. Exosomal RNA was successfully isolated from the media of all 16 cell types. RNA was produced from exosomes and was of sufficient quantity and quality for Q-RT-PCR. The initial PCR with mir16 primers confirmed the presence of cDNA in 6 of the 16 cancer samples. Further results are pending.

Acknowledgments. Funding for these studies was provided by AURIC.

Environmental Sampling for *Salmonella* in an Equine Reproduction Center

Mackenzie T. Michaels[1], Steven R. Kitchens[1], and Stuart B. Price[1]
[1]Department of Pathobiology, College of Veterinary Medicine, Auburn University, AL

Introduction:
Previous studies conducted at the Auburn University College of Veterinary Medicine (AUCVM) found *Salmonella* in the environment of locations proximal to the Equine Reproduction Center (ERC) on the AUCVM campus. This study was conducted to determine if *Salmonella* also was present in the ERC, suggesting proximal movement of the pathogen. Information from this study could be applied to the development of specific interventions to reduce the prevalence and movement of *Salmonella* through the environment of equine reproduction centers.

Methods:
Over the course of this study, multiple sampling methods were utilized to collect environmental samples over a five-week period. Facility samples were taken using pre-moistened 4x4 gauze pads and grab sampling. Pasture samples were taken using pre-moistened 4x4 gauze pads and pooled grab sampling. Water samples were taken using 60-cc syringes. All samples, once collected, were placed in individual 118-mL Whirl-Pak bags and transported back to the lab. A modified protocol from the USDA/FSIS/OPHS Microbiology Laboratory Guidebook's *Isolation and Identification of Salmonella from Meat, Poultry, Pasteurized Egg, and Catfish Products and Carcass and Environmental Sponges* was used to isolate *Salmonella* from the environmental samples. Positive *Salmonella* colonies were serogrouped using antiserum E, K, C_1 or C_2 and serotyped by Biovet, Inc. A data collection form was developed to record important information about each sample to aid in statistical analysis. Statistical Analysis System (SAS) was used to generate frequency tables for the independent variables in regards to the dependent variable (*Salmonella* positive or negative). Epi Info 7.2 was used to calculate the Risk Ratio of the independent variables using a 2x2 contingency table.

Results:
Of the 131 total samples collected from the environment of the ERC at AUCVM, 105 samples were collected prior to interventions being implemented and 26 were collected after intervention implementation. Forty-one percent of the 105 samples collected prior to interventions were positive for *Salmonella* and 23% of the 26 samples collected after interventions were positive for *Salmonella*. Prior to interventions being implemented, there were five independent variables that were shown to be at risk for environmental contamination of *Salmonella*. After the interventions were implemented, there were two independent variables that were shown to be at risk for environmental contamination of *Salmonella.* All but one of the samples contained one or more of *Salmonella* serotypes Muenster, Cerro, or Muenchen.

Conclusions:
The finding of *Salmonella* in the environment of AUCVM's ERC suggests that there was environmental contamination occurring, perhaps shed from one or more *Salmonella* positive horses at the ERC. Interventions put in place during the study reduced the prevalence of *Salmonella* in the environmental samples tested. Two of the serotypes found in the environment (Muenster and Cerro) were previously found in the CVM dairy herd located proximally to the ERC. Although direct transfer between bovine and equine species has not been proven in this study, separation of infected animals from uninfected animals, and enforcement of strict biosecurity measures, are two steps that could be taken to decrease proximal transfer of *Salmonella* in this mixed animal species environment.

Acknowledgments:
Special thanks to Dr. Aime Johnson, Dr. Jennifer Taintor, Dr. Erin Groover, Dr. James Wright, Jessica Brown and Seth Kochera as well as the AUCVM Large Animal Teaching Hospital. This work was supported by The Alabama Agricultural Experiment Station.

Veterinary Student Poster Presentations

Lipopolysaccharide Priming of Equine Mesenchymal Stem Cells

Lindsey H. Boone DVM, PhD, DACVS-LA[1], Brooke M. Alnwick, Satyanarayana R. Pondugula, DVM, PhD[2]
[1]Department of Clinical Sciences, College of Veterinary Medicine, Auburn University, AL
[2]Department of Anatomy, Physiology and Pharmacology, College of Veterinary Medicine, Auburn University, AL

Introduction.
Mesenchymal stem cells (MSCs) exposed to an inflammatory environment can undergo immunogenic or immunomodulatory phenotypic transformation. This initial interaction with an inflammatory environment typically results phenotypic transformation via activation of toll like receptors (TLRs). Lipopolysaccharide (LPS) is a common pathogen released during systemic inflammation and is the ligand of TLR 4. The objective of this study was to evaluate how TLR4 signaling affects immunomodulation of equine bone marrow derived mesenchymal stem cells (BMSCs).

Methods.
Equine BMSCs were treated with 10ng/mL, 50ng/mL, and 100ng/mL LPS and cultured for 1 hr or 24 hrs, at which point the media was removed and standard culture media was added. Cells were cultured for an additional 24 hours post-treatment. Total RNA was extracted from BMSCs using the EZNA total RNA kit, cDNA was synthesized with iScript cDNA synthesis kit. Primers and probes were designed with commercial software. PerfeCTa SYBR Green Kits were used to measure relative expression. mRNA expression was normalized to two internal mRNAs (SDHA and HPRT1). Relative expression was calculated by the comparative threshold cycle (ΔΔ method), and the fold change relative to controls were calculated. Expression of genes (TLR4, MHCII, IL-6, IL-8, IL-10, CCL2, COX2, CXCL10, IDO, and Jagged-1) was reported.

Results.
CCL2 and COX-2 were upregulated after after 1 hr of incubation with 10 ng/ml LPS and IL-6 was upregulated only in one cell line. One hour incubation at 50 and 100 ng/ml caused upregulation of CCL2 and COX2 and downregulation of Jagged-1 expression. CXCL10 was also upregulated after 1 hr incubation with 50 ng/ml LPS where as IL-6 and IL-8 was upregulated after 1 hr incubation with 100 ng/ml LPS. After 24 hour incubation with 10ng/mL LPS resulted in varied individual gene expression between cell lines with upregulation of COX-2 and IL-6 in one horse and upregulation of CCL2 and IL-8 in another cell line. The 24 hour 50ng/mL LPS treatment caused increased gene expression of CCL2 and IL-6. At 24 hour 100ng/mL LPS treatment caused increase in CCL2, COX-2, and IL-6 and decreased Jagged-1 expression.

Conclusions.
In a 2012 study published by Betencourt, Increased CCL2 and CXCL2 are supportive of an immunomodulatory phenotype while increased IL-6 and IL-8 expression are supportive of an immunogenic phenotype in human MSCs. COX-2 is an enzyme that produces prostaglandin E2 (PGE2), which is the major immunomodulatory factor in horses. After 1 hr incubation with 10 ng/ml immunomodulatory genes were upregulated and only the immunogenic gene, IL-6 was upregulated. Further work is needed to understand LPS priming in equine BMSCs and the production of an immunomodulatory BMSC phenotype.

Acknowledgements
Brooke Alnwick would like to thank Boehringer Ingelheim for the opportunity to participate in the veterinary scholars program.

Arming a conditionally replicating canine adenovirus (ICOCAV15) with canine *mda-7* for cancer therapy

Natalie Heape[1], Jonathan Marable[2], Damien Ruiz[2], Maninder Sandey[2]

[1]College of Veterinary Medicine, Auburn University, AL
[2]Department of Pathobiology, College of Veterinary Medicine, Auburn University, AL

Melanoma is the most common malignant oral neoplasm in dogs. Canine oral melanoma (OM) is characterized by a highly aggressive biological behavior with rapid progression from localized to advanced-stage disease. Current treatment strategies, including surgery and radiation therapy, provide transient relief from the local disease. However, chemotherapy or the Oncept vaccine yield no tumor control for the metastatic disease (<3 months median survival for stage III). Thus, alternative therapeutic approaches are needed for the control of primary and metastatic oral melanoma. Oncolytic viruses have been a focus of research as an alternative therapeutic approach to chemotherapy for treating a variety of cancers. Conditionally replicating adenoviruses are genetically engineered to replicate only in cancer cells. ICOCAV15 is a canine adenovirus serotype 2 based conditionally replicating adenovirus (CRAd) that replicates efficiently and selectively in tumor cells. However, ICOCAV15 and its variant, ICOVAV17 had only limited success in a clinical trial when tested in canine patients. Thus, the goal of the present study is to enhance the tumor-killing activity of the ICOCAV15 by arming it with canine melanoma differentiation associated gene-7/Interleukin-24 (canine mda-7/IL-24). In our lab, we have previously shown that ectopic expression of canine mda-7/IL-24 selectively induces growth suppression and cell death in a variety of cancer cells, while simultaneously not harming normal cells. Canine mda-7/IL-24 is a secreted protein and can inhibit the growth of tumor cells by "bystander activity" through its cognate receptors. To create the canine mda-7 expressing ICOCAV15, the open reading frame of the canine mda-7/IL-24 gene was amplified and cloned either in the E3 region or in a region immediately downstream to the ICOCAV15 fiber. To generate the recombinant viruses, we performed the selection, amplification, and homologous recombination in yeast (Saccharomyces cerevisiae, YPH857). The recombinant plasmids were sequenced to confirm the successful cloning of canine mda-7 or dsRed sequences in the E3 region or in the region downstream of the ICOCAV15 fiber. Future studies will involve the amplification and purification of the recombinant viruses. Expression of the dsRed and canine MDA-7 proteins will be confirmed by fluorescent microscopy and western blot analysis, respectively. The antitumor activity of the recombinant viruses will be evaluated by several assays including MTT and apoptosis assays.

Acknowledgments: Dr. Payal Agarwal, Dr. Bruce F. Smith, Dr. Ramon Alemany, Cynthia Hutchinson, Boehringer Ingelheim and the Veterinary Summer Scholars Program.

Effects of Auditory Environment on Dogs during Abdominal Ultrasound Examination.

Amanda Hill, Rachel Moon, Jeanie Roberts, Robert Kemppainen, James Wright, Amelia White, Stephanie Carter, and Elizabeth Gerondale.

Department of Radiology, Auburn University College of Veterinary Medicine, Auburn University, AL

Introduction. Abdominal ultrasound is an increasingly used diagnostic tool in small animal medicine. The aim of this study was to evaluate the effect of the auditory environment on the stress levels of canines during abdominal ultrasound. Specifically we were interested in if (and what type of) music played during the ultrasound procedure had an influence on behavioral and physiologic parameters in normal canines.

Methods. Four healthy beagles were ultrasounded twice weekly for a total of four weeks. Three ultrasound sessions were performed in the absence of auditory stimulation. During the other five sessions each dog was subjected to music of different types (classical, country, techno/trance, reggae, alpha waves). Pre and post salivary cortisol was collected daily from each dog. Heart rate (HR) and heart rate variability (HRV) parameters (including RR interval, PNN50) were assessed with a Polar heart rate monitor (H7; Polar, Kempele, Finland). Subjective parameters of stress level were evaluated by the canine handlers and ultrasonographer and a consensus score (1-5) recorded.

Results. A significant increase in PNN50 ($P=0.042$) was noted during the playing of country music versus the absence of music. There were also positive trends in the PNN50 during the playing of reggae and alpha waves however these were not found to be statistically significant. Classical music and techno/trance auditory stimulation showed negative trends in HR, mean RR and PNN50 compared to no music stimulation. The auditory environment had no statistically significant effects on salivary cortisol measurements.

Conclusion. Results of this study show promise that modifications of the auditory environment can decrease stress levels in dogs during abdominal ultrasound examination. Further investigations utilizing larger sample sizes and variety of auditory stimuli may identify simple and economic environmental adjustments to decrease stress in canine patients during imaging procedures.

Mutational analysis of the Factor XIIIa gene in a Poodle with Factor XIII deficiency.

Brooklyn Isaacs[1], Marjory B. Brooks[2], Kevin B. King[1], Mary K. Boudreaux[1] and Pete W. Christopherson[1]

[1]Department of Pathobiology, Auburn University College of Veterinary Medicine, Auburn University, AL
[2]Department of Population Medicine and Diagnostic Sciences, Cornell University College of Veterinary Medicine, Ithaca, NY

Introduction. Factor XIII deficiency has been described in people and one Poodle. This condition results in the inability to crosslink fibrin which is essential for the formation of a firm, fibrin clot during the final stages of coagulation (secondary hemostasis). Patients can have lifelong bleeding tendencies and delayed wound healing. This deficiency is most often inherited, but acquired deficiencies have been associated with some human diseases. Factor XIII is an enzyme that circulates as an inactive tetramer in blood; it is comprised of two catalytic A subunits and 2 carrier B subunits. It is activated by thrombin with calcium an essential cofactor. Factor XIII is encoded by the Factor XIII-A1 (F13A1) and Factor XIII-B (F13B) genes. Genetic analysis of people with congenital Factor XIII deficiency have shown causative mutations are predominantly found in the F13A1 gene. Patients presenting with Factor XIII deficiency have clinical bleeding with normal platelet counts, platelet function tests, coagulation times, functional fibrinogen, and von Willebrand factor (vWF) antigen levels. The purpose of this study is to determine the mutation responsible for causing Factor XIII deficiency in a 1-year-old, male Poodle that had prolonged bleeding following castration and a left hindlimb lameness partially due to a chronic hematoma.

Methods. Initial diagnostics including a CBC, coagulation panel, fibrinogen concentration, and vWF antigen levels were performed. Additional diagnostics included platelet aggregation testing, a reptilase test for dysfibrinogenemia, a clot stability test, and factor XIII activity assay. Genomic DNA from this patient was isolated from whole blood and subjected to PCR to amplify the coding regions of the factor XIIIa gene (F13A1). Additional primer sets were designed in the non-coding regions of the gene to sequence areas of introns 6 and 8. Results were compared to both normal dog sequence and canine GenBank sequence.

Results. Platelet count, coagulation testing, vWF antigen, platelet function, and dysfibrinogenemia tests where all within normal limits. Results of a clot stability test were consistent with severe factor XIII deficiency with the control clot being stable for >24 hours, while the patient's clot dissolved in <30 minutes. Factor XIII activity assay results found no detectable factor activity. Sequencing of 13 of 15 coding exons matched with controls and GenBank sequence. Exons 7 and 8 failed to amplify repeatedly, while primer sets worked with control DNA. Intronic sequencing narrowed the mutation location to within the region that includes the last ~5,000 bases of intron 6 through the first 3,400 bases of intron 7.

Conclusion. This case is the second clinical description of Factor XIII deficiency in a Poodle and the first reported attempt to identify an underlying mutation in the F13A1 gene. The initial results of this study suggest a large deletion present in the area of the F13A1 gene that includes exons 7 and 8. Further work is needed to determine the exact mutation associated with Factor XIII deficiency in this patient. Factor XIII deficiency should be a diagnostic consideration for veterinary patients with clinical bleeding, particularly coagulation-type hemorrhage, that have normal platelet numbers, platelet function, routine coagulation tests, and von Willibrand factor antigen levels.

A Case of Necrotizing Purulent Pleuropneumonia in a White-tailed Deer

Samantha N Weatherford[1], Cary Laster[2], Johna Veatch[3], Debbie Reed[4], Lindsay Starkey[5]
[1]Breathitt Veterinary Diagnostic Laboratory, Hopkinsville, KY
[2]Auburn College of Veterinary Medicine, Auburn University, AL

Introduction

A ~1 year old male White-tailed deer was presented at Breathitt Veterinary Center for necropsy on the morning of May 17, 2018. The animal was found dead in a cattle feedlot in Western KY and the owners requested that Kentucky Fish and Wildlife transport it to Breathitt Veterinary Center. Feedlot owners were concerned about the deer spreading disease to the cattle. The Kentucky Fish and Wildlife Officer requested the deer be tested for: Chronic Wasting Disease, tick-borne diseases and that a cause of death be determined.

Methods

Grossly, the animal was in poor body condition with a body score of 1 out of 5. The hair coat was rough and numerous ticks were noted, especially around the base of the ears and the perineal region. A reddish brown fluid drained from the nares. Internally, lungs were adherent to the thoracic wall. The left lung had multifocal abscesses with destruction of normal tissue while the right lung was not as severely affected. Round worms and whipworms were present in the large intestine. Samples of tissues were submitted for bacterial culture, epizootic hemorrhagic disease testing, fecal exam, and chronic wasting disease testing. Ticks were submitted to the Auburn College of Veterinary Medicine's Department of Parasitology for identification. A 4dx snap test was also performed to determine if the deer harbored any tick-borne diseases. Fixed tissue samples were prepared for histopathological slides.

Results

In the histopathological slides of the lung, *Dictyocaulus viviparous* larvae were observed. Bacterial cultures of lung abscesses were determined as *Trueperella pyogenes*. The results of the 4dx snap test indicated that the deer was a faint positive for *Ehrlichia chaffeensis*. Both tests for CWD and EHD were negative. Necrotizing purulent pleuropneumonia was determined as the morphological diagnosis for the deer.

Conclusions

The deer's cause of death was due to parasitism and severe pneumonia. With the exception of the lungworms, the animal did not harbor disease that would infect the cattle.

Acknowledgements

Dr. Dan Givens, Dr. Lindsay Starkey, Dr. Debbie Reed, Dr. Johna Veatch, Dr. Cary Laster
Boehringer Ingelheim's Summer Scholars Program
The Office of Research and Graduate Studies at Auburn College of Veterinary Medicine

Cannabinoid Receptor Quantification in Normal and GM1 affected Feline Tissues

Krista B. Wood, Kamoltip Thungrat, Dawn M. Boothe
Department of Anatomy, Physiology, and Pharmacology, College of Veterinary Medicine, Auburn University, Al

While there has been a wide range of interest in using various cannabinoids derived from *Cannabis sativa* to treat multiple illnesses in Veterinary medicine the distribution of the cannabinoid receptors in veterinary species has not been fully evaluated. Our objective was to characterize cannabinoid receptor 1 (CB1) and cannabinoid receptor 2 (CB2) in normal cats and cats affected with GM1 and compare these expression levels with housekeeping genes in order to quantify each receptors genetic expression. Tissue samples were collected from three healthy cats and three GM1 affected untreated cats whose ages ranged from 6.8 months to 8.2 months. Each group contained two males and one female. From each cat we collected cortex, liver, gonad, spleen, lung, thymus, spinal cord, small intestine, kidney, and mesenteric lymph node. These tissues were used for RNA extraction and qPCR. We used Beta-actin and ABL as reference genes. A t-Test two sample assuming unequal variances was used to analyze the qPCR results after normalizing the data acquired to the reference gene data before comparing between healthy and GM1 affected cats. The gene expression of CB1 and CB2 were quantifiable but our results were not statistically significant. The small intestine had little to no quantifiable expression of CB2 but it is unclear at this time if this is a repeatable finding or an error from the small sample size or other methodology. Our future research will include expanding our sample size, utilizing Western blotting, and using IHC to characterize the distribution of these receptors.

Acknowledgements: K. Thungrat DVM, PhD, D. Boothe DVM, MS, PhD, Meador-Woodruff Laboratory, Boehringer Ingelheim Veterinary Scholarship.

Graduate Student Poster Presentations

A Synopsis of Neoplasms Diagnosed in Backyard Chickens Submitted to the Alabama Department of Agriculture and Industries Veterinary Diagnostic Laboratory System, 2016-2017

Erfan Chowdhury[1, 2], John Roberts[2], Tami Kelly[1], Terry Slaten[1], Laurie McCall[1], Sara Rowe[1], Lanquing Li[1], Kellye Joiner[2] and Heather Walz[1]

1 AL Department of Agriculture and Industries, Veterinary Diagnostic Laboratory system
2 Department of Pathobiology, College of Veterinary Medicine, Auburn University, AL

Introduction: The records of Alabama Department of Agriculture and Industries, Veterinary Diagnostic Laboratory system (ADAI-VDL) from January 1, 2016 to December 31, 2017 were analyzed to determine the prevalence and type of neoplastic diseases that were diagnosed system wide. An overview of this retrospective study is presented here.

Methods: All necropsies were performed according to the standard operating procedures of ADAI-VDL. In every case, a complete necropsy was performed, visible gross findings were identified, and samples were collected for further laboratory analysis. Collected tissues, blood, and swab samples were analyzed through bacterial culture, ELISA, PCR, cell culture, and histopathology.

Results: From 2016 to 2017, a total of 348 backyard poultry cases were submitted to the ADAI-VDL. Off those submission, neoplastic diseases were diagnosed in 105 (30% of total) cases. Among different neoplasms, Marek's disease (MD) was diagnosed in 85 (24% of total) and adenocarcinoma in 18 (5%) cases. Sarcoma, fibrosarcoma, leiomyosarcoma, and teratoma were diagnosed at 1 of each. In case of MD, lymphoma or lymphatic infiltration was observed in multiple visceral organs including lung, liver, kidney, intestine, ovary, and oviduct, with or without neural involvement. The adenocarcinoma was mostly ovarian origin, however in some cases the primary source could not be precisely determined.

Conclusions: The finding of this study clearly demonstrates that neoplastic diseases are the most common cause of death in backyard chicken. Among various neoplasms, MD is the most prevalent. MD is highly controlled in commercial chickens due to vaccination but BY chickens are rarely vaccinated against this disease. Therefore, with the current increases in BY flock numbers there is an increase in susceptible chickens which can easily get infection through contact of infected chickens or contaminated environment.

Evaluation of two methods to collect canine melanocytes

Taylor D. Flaat[1], Payal Agarwal[1], Rebecca Nance[1], Paulina Platton[3] and Bruce F. Smith[1,2]

[1]Department of Pathobiology, College of Veterinary Medicine, Auburn University, AL
[2]Scott-Ritchey Research Center, College of Veterinary Medicine, Auburn University, AL
[3]Texas A&M College of Veterinary Medicine and Biomedical Sciences, College Station, TX

Introduction. One of the most difficult aspects of employing precision medicine in the treatment of cancer is determining the best targets to treat within the tumor. A trademark of cancers is that while two patients may present similar tumors of the same tissue, even at the same stages of development, they will likely not respond in the same way to identical treatment. This issue is common throughout all types of cancers and presents a significant hurdle in creating effective treatment regimens for patients. Melanoma is a significant tumor of dogs that typically occurs in the oral mucosa. Normal melanocytes from canine melanoma patients are needed to compare transcriptomes to patient melanomas using deep sequencing and from this data, therapeutic targets may be selected. The current project seeks to identify and obtain appropriate normal melanocytes from patient animals with minimal additional morbidity. Epidermal melanocytes represent a population of approximately 3-7% of a cell types throughout the skin, making them a difficult target to isolate. Herein, we evaluate two potential methods for the isolation of pure canine melanocytes from normal skin.

Methods. The first method is a differential adhesion method using cell culture. Briefly; punch biopsies from normal canine skin were incubated overnight in dispase. After incubation the epidermis was separated from the dermis and treated with trypsin EDTA or 1x TrypLE recombinant trypsin to disperse the epidermal cells into a single cell suspension and cultured in Melanocyte Growth Medium M2. Method two involves the plucking of anagen hair follicles from normal dog skin for explant culture. Approximately 80-100 hairs were plucked from the dorsocranial region of healthy dogs under non-sterile conditions and 30-50 anagen hairs with attached follicles were selected under a microscope. The hairs were washed in melanocyte Growth Media before explanting 12-15 follicles onto each microporous membrane in Melanocyte Growth Medium. Cells were cultured under normal cell culture conditions.

Results. Method one resulted in the isolation of identifiable melanocytes from non-haired oral mucosa. Thus far pure cultures of melanocytes from haired skin have not been isolated by this method. Method two has also not resulted in the isolation of identifiable melanocytes.

Conclusions. The isolation of melanocytes from oral mucosa, while possible, is not practical in patients already undergoing significant oral resection for tumor. Unfortunately, published methods of isolating melanocytes from haired regions of the dog, either by punch biopsy or follicle isolation, has not yet proven feasible. The largest issue to date is that hair follicles act as anchors for the epidermis in normal canine skin making separation from the dermis difficult. We are employing different alterations to attempt to overcome this hurdle as well as looking into alternate isolation methods.

Acknowledgments. – Funding for this study was provided by AURIC and the Office of Research and Graduate Studies (Flaat).

High Performance Liquid Chromatography-UV Detection and Validation of Primaquine phosphate in Penguin Plasma

[1]Christina Hargis, [1]Crisanta Cruz-Espindola, [1]Dr. M Boothe
[1]Department of Anatomy, Physiology, and Pharmacology, College of Veterinary Medicine, Auburn University, AL

Introduction: Primaquine diphosphate (PQ) is an 8-aminoquinoline antimalarial drug. It is a commonly used drug to treat and prevent malarial infections in penguin zoo populations. Proper use of any antimicrobial should be based on pharmacokinetic studies that support proper doses in that species. However, no published validated method exists for the extraction and quantitation of PQ plasma concentrations in penguins. Without this information veterinarians cannot establish appropriate doses necessary to target malaria or monitor plasma concentrations in penguins. In this study a high performance liquid chromatography method with ultraviolet detection (HPLC-UV), including protein precipitation extraction (PPE), was developed and validated for PQ in penguin plasma.

Methods: Several different stationary phases and mobile phases were tested to determine optimal conditions for analyzing PQ with HPLC-UV. Several methods of extracting the drug from penguin plasma were tried due to the complexity of the plasma, in part because the penguin diet consisting primarily of fish, and the overall instability of PQ. Included among the many methods of extraction tested were: solid phase extraction (SPE), liquid-liquid extraction (LLE), PPE, PPE followed by drying with nitrogen (N_2) to concentrate the sample, and finally PPE followed by incubation then drying with N_2. The latter method provided for the best precision and accuracy of PQ detected and quantitated in penguin plasma, while also increasing the stability of PQ during the extraction process.

Results: PQ was extracted from penguin plasma using PPE, followed by a 60 min incubation period at 60°C, then drying with N_2 and reconstitution of the sample in mobile phase. Samples were analyzed by Reverse Phase HPLC-UV with a Luna C18 column (150mm x 4.6 i.d. x 5 µm) as the stationary phase, and a mixture of 0.1% phosphoric acid in water and methanol as the mobile phase. The flow rate was 0.8 ml/min, and column temperature set at 40°C, and UV absorbance measured at 264 nm. The method was validated for linearity, accuracy, and intra-day/inter-day precision. The linear coefficient for PQ in penguin plasma was 0.99. The limit of detection (LOD) and lower limit of quantification (LLOQ) were 15 ng/ml and 20 ng/ml respectively. The Precision (CV %) for PQ in penguin plasma 25, 60, 125 and 350 ng/mL was 3.25%, 7.69%, 4.79%, and 8.07% respectively. The Accuracy (% Recovery) for PQ in penguin plasma 25, 60, 125 and 350 ng/mL was 112.66%, 102.86%, 92.64%, and 92.16% respectively. The overall stability of PQ after extraction from the plasma was found to be 16 hours before significant degradation began to occur.

Conclusions: The new validated method is suitable for detection and quantification of PQ in penguin plasma concentrations to help veterinarians accurately dose penguins for the treatment and prevention of malaria in zoo populations, and ultimately establish therapeutic ranges.

Acknowledgements: Department of Anatomy, Physiology, and Pharmacology. Dr. M Boothe, Crisanta Cruz-Espindola, Benjamin Driggers. The Maryland Zoo in Baltimore.

Effects of soy isoflavones on Leydig cell steroidogenesis

Bamidele O. Jeminiwa[1], Rachel C. Knight, John F. Fischer, Samantha M. Bradley and Benson T. Akingbemi[1]

[1]Department of Anatomy, Physiology and Pharmacology, College of Veterinary Medicine, Auburn University, AL 36849.

Introduction. The general population is exposed to isoflavones through the consumption of soybeans and other legumes. Children, especially neonates and infants, are exposed to high doses of isoflavones in soy-based formulas. For example, 250,000 infants are raised on soy formulas annually in the United States. Genistein and daidzein are the major isoflavones found in soybeans. Previous studies from our lab and others have shown that genistein possesses hormonal activity and may interfere with male reproductive development. However, it is not clear that effects of soy-based diets on testicular function are due to singular or combined actions of isoflavones.

Methods. We determined effects of isoflavones on androgen biosynthesis using primary Leydig cells isolated from 35-day old Long-Evans male rats. Leydig cells were incubated in DMEM/F12 culture media in the presence of 10 ηg/mL ovine LH and increasing concentrations of genistein, daidzein and equol. Testosterone secretion by Leydig cells was measured in aliquots of spent media by radioimmuno assay.

Results. Results showed that genistein inhibited testosterone production in a concentration-dependent manner (control: 225±15, 0.01 μM: 194±15, 0.1 μM: 155±15, 1 μM: 124±15, 10 μM: 157±15 ηg/10^6 cells; $p<0.05$). The timing of onset of genistein inhibition was determined to be 10 h (control: 216±5 versus genistein: 166±5 ηg/10^6 cells; $p<0.05$). However, genistein inhibition of Leydig cell testosterone production was reversed 8 h post-treatment (control: 87.5±5 versus genistein: 87.5±5 ηg/10^6 cells). In a repeat experiment, Leydig cell testosterone production was suppressed after 18 h incubation with genistein (1 μM) but not with daidzein and equol (control: 105±5 versus genistein: 76.5±5; $p<0.05$; control: 84±5 versus daidzein: 91±5; control: 80±5 versus equol: 81±5 ηg/10^6 cells; $p>0.05$).

Conclusions. Results suggest that genistein exerts a direct inhibitory effect on Leydig cells testosterone production. However, animal studies are required to determine if genistein, daidzein and/or equol affect other levels of the male reproductive axis.

Acknowledgments. Funding for this research was by NIH grant ES 158882-02.

Flow cytometry analysis of Mammaglobin-A in canine mammary tumor cell lines.

Gisela Martinez-Romero[1], Patricia DeInnocentes[1], R. Curtis Bird[1]
[1]Department of Pathobiology, College of Veterinary Medicine, Auburn University, Auburn, AL

In our laboratory we have explored the expression profile of Mammaglobin-A (MGBA) in canine breast cancers, which is considered a target for cancer vaccine therapy. The first approach to analyze the expression of MGMA in canine tumors indicated that this gene was expressed in five established canine mammary tumor (CMT) cell lines and phenotypically normal canine mammary epithelial cells (CMEC). The aim of the present study was to analyze the expression of Mammaglobin-A by flow cytometry.
Five established canine mammary tumors cell lines (CMT 12, 27, 28, 47, 119) and CMEC cells were grown in Alpha-MEM supplemented with 10% FCS, 100U/ml penicillin, and 100µg/ml streptomycin. Total cellular RNA was extracted from the cell lines using the High Pure RNA isolation kit according to the manufacturer's instructions. RNA was next analyzed by reverse transcriptase-PCR (QrtPCR) using the Access RT-PCR system according to the manufacturer's instructions. The forward primer for mammaglobin-A was 5'-ATGAAGCTGCTGAGAGTCCTTGTGCTG-3' and the reverse primer was 5'-GCAAAATTGCTCAGAGTTTCATCCGA-3. CMT12 and CMT119, cells lines with the highest gene expression, were analyzed with flow cytometry using a MGBA polyclonal antibody. MGBA antibody was raised in rabbit (Abbiotec, San Diego, CA), using a synthesized peptide derived from canine MGBA as the immunogen. For intracellular flow cytometry, cells were fixed and permeabilized using the Fixation and Permeabilization kit *(*eBioscience, SanDiego, CA*).* Cells were incubated with primary anti-MGBA antibody labeled with Zenon Alexa fluor 488. The samples were analyzed on a Cytoflex LX flow cytometer. In all CMT cells and the CMEC cell line, the expected 237 bp fragment was detected on ethidium bromide-stained agarose gel. All analyzed CMT cell lines had variable increased expression levels of MGBA when compared with CMEC cells. By flow cytometry, we found that MGBA expression on CMT cells was 2-3 fold higher than CMEC. The low level of Mammaglobin-A gene expression and the high levels of fluorescence in CMEC cells could be attributed to differences in Mammaglobin-A protein half-life or translation efficiency.

Acknowledgments: The authors thank AURIC for funding, and Allison Church Bird and Farruk Lutful Kabir for valuable collaboration and consultations.

Tonsillar biopsy for routine staging of non-tonsillar primary oral tumors: Assessment of complications and evidence of disease in 28 cases

Keiko Murakami[1], Nicholas J. Rancilio[1], Jeannie M. Poulson[2]

[1]Department of Clinical Sciences, Auburn University, AL

[2]College of Veterinary Medicine, Purdue University, IN

Introduction: It is known that the tonsil is one of the sites that primary malignant oral tumor metastases in dogs. Local treatment such as surgery and/or radiation therapy (RT) is a major treatment option in dogs with oral tumors. The metastasis in the tonsil may significantly impact on the treatment recommendation and prognosis. However histologic evaluation of the tonsil is not routinely performed in dogs with oral tumors unless it is grossly abnormal.
The purposes of this study was to assess the complications associated with the tonsillar biopsy and evidence of disease in 28 dogs with non-tonsillar primary oral tumors.

Methods: Client-owned dogs with non-tonsillar primary oral tumor that underwent tonsillar biopsy were evaluated. The tonsillar biopsy was performed with Jackson uterine biopsy forceps under general anesthesia. Dogs with primary tonsillar tumor were excluded. Through oral examination and assessment of the tonsil under general anesthesia or heavy sedation was performed prior to tonsillar biopsy. Follow up examination were performed approximately 1 week after the procedure in most cases.

Results: Twenty-eight client owned dogs that had non-tonsillar primary oral tumor were evaluated for the incidence of metastasis in the tonsil. There were fourteen oral squamous cell carcinomas, five oral malignant melanomas (OMM), two oral sarcomas, two fibrosarcomas (FSA), and one of each atypical acanthomatous ameloblastoma, plasmacytoma, malignant peripheral nerve sheath tumor (PNST), granular cell tumor, and 2 inconclusive tumors such as PNST vs. FSA, and spindle cell tumor vs. OMM.
The tonsillar biopsy procedure was quickly and easily performed by clinicians. It took approximately 3-5 minutes to control the local hemorrhage with hand-compression with gauze after the biopsy. The hemorrhage was not significant issue for any of our patients.
The incidence of metastasis in the tonsil was 13.7%. Results of the oral examination was available in 24 cases. Among of these patients, 16.7% (4/24 cases) had a grossly abnormal tonsil with the thorough oral examination.
None of the patients had clinically significant complication after the procedure.

Conclusions: Tonsillar biopsy as part of routine staging examination for various oral tumors is a safe procedure that can be done under heavy sedation or general anesthesia. Occult neoplastic disease may be present in the tonsils despite a grossly normal tonsil. The incidence of tonsillar metastasis in dogs with non-tonsillar primary oral tumor was 13.7% in our study. It may be beneficial to include tonsillar biopsy as a routine staging examination in dogs with primary oral tumor due to the low risk of complications. However further evaluation in a bigger population will be warranted.

Complexities of familial cancer risk - investigating a large African American family

Sophonie M. Omeler[1], Madison R. Bishop[2], Anna LW Huskey[2], Nancy D. Merner[1]
[1]Department of Pathobiology, College of Veterinary Medicine, Auburn University, AL
[2]Department of Drug, Discovery and Development, Harrison School of Pharmacy, Auburn University, AL

Introduction. African-Americans (AA) make up a breast cancer (BC) population that is widely understudied due to barriers such as mistrust of researchers and lack of accessibility to institutions providing these research opportunities. Though BC incidences have converged between ethnicities, the incidence is still higher in AA women below the age of 40, a hallmark of hereditary BC. Additionally, it is typically observed that AA women have a higher mortality rate at every age and are typically diagnosed with triple-negative breast cancer, a more aggressive breast cancer subtype. Despite federal mandates to include minorities in studies that rely on federal funding, there are still disparities in research. Knowing this, the Merner lab set out to reach underrepresented women throughout the state of Alabama through a community-based recruitment (CBR) program. It is through this recruitment method that Family 1CAD was recruited into our study.

Methods. Members of Family 1CAD (n=13; 4 BC-affected, 1 ovarian cancer-affected, and 8 cancer-unaffected individuals) were recruited and enrolled through the CBR recruitment protocol. Through CBR, it was disclosed that a deceased family member had a *BRCA1* mutation (p.M1796R). Therefore, all participating family members were screened for the *BRCA1* mutation through polymerase chain reaction (PCR) and Sanger sequencing (SS); only three cancer-affected individuals screened positive. Additionally, the five cancer-affected family members were screened using a targeted gene panel, B.O.P. (Breast, Ovarian and Prostate) along with 131 other individuals in the Alabama Hereditary Cancer Cohort (AHCC). This screening corroborated the *BRCA1* mutation status in Family 1CAD and identified additional variants; variants of interest were subsequently validated through PCR and SS. AA breast cancer data from The Cancer Genome Atlas (TCGA) was used to validate our findings. Exome Variant Server (EVS) served as ethnic-specific controls.

Results. B.O.P. capture and sequencing revealed that the three members of Family 1CAD who carry the familial *BRCA1* (p.M1796R) mutation also harbor a truncating *MAD1L1* (p.S40fs) mutation. Two unrelated AA probands from the AHCC also had the same *MAD1L1* mutation; interestingly, they also carried a *BRCA1/2* variant. Aggregation analyses using TCGA and EVS revealed that *MAD1L1* truncation variants are associated with BC in AAs under the age of 45 (P=0.02).

Conclusions. The genetic analysis of Family 1CAD reveals a complicated story. Some individuals' cancer-risk are explained by a *BRCA1* mutation and others' not. Furthermore, B.O.P. sheds light on polygenic risk; a *MAD1L1* truncation mutation was identified in the *BRCA* mutation carriers in the AHCC. Further investigation suggests that *MAD1L1* truncation mutations are associated with early onset AA BC. Therefore, individuals with a *MAD1L1* truncation variant have a genetic predisposition to breast cancer, likely working in conjunction with variants in other susceptibility genes, such as *BRCA1*.

Acknowledgments. We thank the College of Veterinary Medicine and Auburn University, as well as our community partners and study participants.

Expression of cannabinoid receptors in human prostate cancer cell lines: A novel pharmacologic target?

Saba Omer[1], Mahmoud Mansour[2], Sabrina van Ginkel[2], and Dawn Boothe[2]
[1]PhD Student, Biomedical Sciences, Auburn University, AL
[2]Department of Anatomy, Physiology, and Pharmacology, Biomedical Sciences, Auburn University, AL

Introduction:
Multiple human tissues express cannabinoid CB1 and CB2 receptors which are G protein couple receptors that can be activated by endogenously released endocannabinoids or exogenously administered cannabinoid agonist compounds, to reduce pain and chemotherapy-induced adverse effects. Recent data suggest anti-proliferative, pro-apoptotic, anti-angiogenic and anti-metastatic activity in several models of cancers including prostate cancer. Purpose of this study is to establish base line expression of CB1 and CB2 cannabinoid receptors in human prostate cancer cell lines, and to investigate the antiproliferative effects of cannabinoid receptor agonists in prostate cancer cell lines.

Method:

Cells: Human-derived DU-145 and PC3 cells were maintained in DMEM complete growth media supplemented with 10% fetal bovine serum and 1% antibiotics. Non-malignant RWPE-1 immortalized human prostatic epithelial cells were maintained in Keratinocyte-SFM complete growth media supplemented with bovine pituitary extract and human recombinant epidermal growth factor.
PCR: Total RNA was isolated from all three cell lines using TRI Reagent (Sigma, St. Louis, MO) according to the vendor's protocol. cDNA was made with iScript cDNA Synthesis Kit (BIO-RAD, Forester City, CA). PCR a Conventional PCR was performed with AcccuStart II PCR SuperMix (Quanta BioSiences (Beverly, MA) and products were visualized using gel electrophoresis method. Primers for CB1 and CB2 were designed by GeneCopoeia, Inc. (Rockville, MD). CB1 and CB2 cannabinoid receptors were amplified using qPCR using PowerUp SYBR Green Master Mix (AppliedBiosystems, Carlsbad, CA).

Results:

Conventional PCR: We found positive expression of CB1 receptors in both prostate cancer cell lines (PC3 and DU145) but CB2 receptors were not found.
qPCR: Results from qPCR confirmed CB1 receptor expression in both normal prostate (RWPE) and cancer cell lines (PC3 and DU145).

Conclusion:

- CB1 receptor were present in RWPE 1 normal prostate cells as well as PC3, DU145 prostate cancer cell lines. In contrast, CB2 receptors were not detected in any of the cells used.
- Expression level of CB1 receptors in normal and prostate cancer cell lines was not significantly different in the absence of endocannabinoid agonists.

Acknowledgements:
Special thanks to Dr.Mansour's lab for sharing prostate cell lines.

CRISPR-CAS9 Mediated Genetic Modification of Canine Adenovirus Type 2

Abdul Mohin Sajib[1], Rebecca Nance [2], Dr. Payal Agarwal[2], Dr. Bruce F. Smith[1,2]
[1]Department of Pathobiology, College of Veterinary Medicine, Auburn University, Auburn, AL [2]Scott-Ritchey Research Center, College of Veterinary Medicine, Auburn University, Auburn, AL

The clustered regularly interspaced short palindromic repeat (CRISPR) along with an RNA-guided nuclease called Cas9 (CRISPR/Cas9) is one of the most powerful tools that has been adopted for precise genome editing in various cells and organisms. Recombinant Adenoviral (Ad) vectors derived from human serotype 2 and 5 are currently the most common vehicle for efficient in vivo transgene delivery and account for 23.8% of nearly 1700 clinical trials that were conducted by using both viral and non-viral vectors. Initial binding of virus fiber knob to the cell surface coxsackie-adenovirus receptor (CAR) followed by secondary binding with $\alpha_v\beta_{3/5}$ integrins on the cell surface are the prerequisites for successful viral internalization to the target cell. However, several studies have shown that cells of lymphocyte origin (B cell, T cell, NK cells etc.) are poorly infected by adenovirus due to the paucity of both CAR and integrins. Hence, retargeted adenovirus must be developed that will bypass both CAR and integrin requirements. Our goal is to explore mechanisms to target lymphocytes at the level of transduction (or infection). Transductional targeting provides improved gene transfer into cancerous cell and spares normal cells. This is typically accomplished through surface modification of the gene delivery vehicle to enhance specific interactions with cancer cell membrane proteins. We hypothesize that transductional targeting of adenovirus by utilizing anti-Interleukin-2-receptor (IL-2R) antibody to target cell surface Il-2R will allow us to conduct CAR and integrin independent cell specific targeting of adenovirus to malignant lymphocytes. However, the conventional approach to modify adenoviral genome is time consuming, complex and less feasible as it is dependent on the presence of unique restriction enzyme sites that may or may not be present in the target site. We propose to utilize in vitro CRISPR/CAS9 mediated editing of the canine adenovirus type 2 (CAV2) genome to promote targeted mutations in viral genome. To achieve this goal, we have successfully inserted the RFP (red fluorescent protein) reporter construct driven by adenoviral major late promoter (MLP-DsRed). This in vitro CRISPR mediated editing of large CAV2 genome exhibits high efficiency and accuracy. Consequently, we are also in the process of utilizing CRISPR/Cas9 technology to replace the wild-type CAV-2 fiber knob domain with interleukin 2 (IL-2) ligand.

Pharmacokinetics of multivesicular liposomal encapsulated cytarabine (DepoCyt™) following subcutaneous administration in dogs

Irene B. Vazquez[1], Annette N. Smith[1], Amanda R. Taylor[1*], Sue H. Duran[1], and William R. Ravis[2]

[1] Department of Clinical Sciences, College of Veterinary Medicine, Auburn University, AL
[2] Department of Pharmacal Sciences, Harrison School of Pharmacy, Auburn University, AL

*Corresponding author: art0022@auburn.edu

Poster presentation;Graduate Studeny, Medical Oncology Resident

Introduction. Meningoencephalomyelitis of unknown etiology (MUE) and lymphoproliferative disorders are commonly observed within the canine population and can be treated with cytarabine (CYT). CYT is a chemotherapeutic drug that exhibits cytotoxic activity specifically during the S-phase of the cell division cycle. For therapy with CYT to be effective, it must be administered intravenously (IV) as a constant rate infusion (CRI) for a sustained period of time. This requires hospital admission and is associated with increased expenses. CYT encapsulated into liposomes may offer an alternative to CRI of the non-liposomal encapsulated form of CYT. Although recently discontinued, DepoCyt™ (DC) was a CYT formulation of multivesicular liposomes labeled for intrathecal administration in people for the treatment of neoplastic meningitis. The primary goal of this study was to determine the pharmacokinetics of DC when administered SQ in dogs.

Methods. A total of 5 healthy female laboratory beagles were utilized in the study in accordance with the IACUC at AU-CVM. During the first study period (SP), two dogs were randomly selected as pilot dogs (PD) to receive DC at 50mg/m2 SQ and the remaining three dogs received free CYT at 25mg/m2 SQ. During the second SP, the PD received free CYT at 50mg/m2 SQ and the remaining dogs received free CYT at 25mg/m2 IV. During the third and last SP, the PD received free CYT at 50mg/m2 IV. Because DC was discontinued, the remaining two dogs were not able to receive it as planned. Washout periods were used between each SP and sampling times. Plasma samples were collected at different points in time and stored at -80°C until analyzed. CYT plasma concentrations were determined using high-performance liquid chromatography and mass spectrometry. Pharmacokinetic analysis was performed using non-compartmental and compartmental analysis using Phoenix® WinNonlin® 64 and Microsoft® Excel. CYT and DC concentration-time profiles were obtained, as well as Cmax, Tmax, AUCinf or AUClast, Cl, t ½, Vd and MRT.

Results. In the PD treated with SQ DC at 50mg/m2, the following mean values were obtained: Cmax was 43.04ng/dL, Tmax was 2h, and the AUClast was 897.4 h*ng/mL. It was not possible to evaluate the remaining parameters as initially planned.

Conclusions. CYT encapsulated into liposomes is very slowly absorbed from the liposomal product when administered SQ, especially when compared to SQ administration of free CYT. Over the first day, 5 to 10% of the administered dose appears in circulation. Only 20 to 30% of the administered dose is present in circulation 10 days after it is administered. The time it takes for DC to achieve its maximum concentration in plasma is much longer when compared to free CYT when administered SQ and IV. At higher doses, more desirable results may be achieved. CYT encapsulated into liposomes may offer an alternative to free CYT.

Acknowledgments. Robert Rusty Arnlold and Jani Lasper for all of their had work help with analyzing the plasma samples.

Comparison of two bandage splint constructs in an ex vivo mid-metacarpal equine fracture model

Kathleen Weatherall[1], J. Dylan Lutter[2], and Warren Beard[2]

[1] Department of Clinical Sciences, Auburn University, AL
[2] Department of Clinical Sciences, Kansas State University, KS

Introduction. In the event of an equine long bone fracture, proper stabilization in the field is key with bandages and splints commonly used by practitioners in the field to transport the horse for continued diagnostics or referral. The true impact of bandage material application in stabilization of equine fractures is minimally understood, due to lack of objective studies evaluating the recommended techniques in an ex vivo or in vivo fashion. We hypothesized that a single stack (SS) bandage with splints would provide similar and adequate neutralization of forces to prevent bending of a metacarpal fracture when compared to the Robert Jones bandage (RJB) with splints, but would result in greater sub-bandage pressure.

Methods. The two bandage types with splints placed in two planes at 90° to each other were applied to 8 equine cadaver limbs with a mid-metacarpal transverse fracture and stability was compared. The constructs were stressed under partial weight bearing load and sub-bandage pressure measured to document stabilization of the fracture by measuring deflection distance and angle.

Results. Results showed mean deflection distance (13.1 ± 2.6 cm [RJB] and 11.4 ± 3.1 cm [SS]) and angle (10.7 ± 3.0 cm [RJB] and 9.8 ± 2.6 [SS]) were not statistically different between the two bandage/split constructs (P = 0.23 and 0.538 respectively). Greater mean sub-bandage pressures were achieved on both the dorsal (102.5 ± 15.0 [RJB] and 125.5 ± 17 [SS]) and lateral (81.5 ± 8.1 [RJB] and 109.3 ± 14.8 [SS]) aspects of MC3 with the single stack bandage when compared to Robert Jones Bandage (P = 0.01 and 0.005 respectively).

Conclusions. The lack of statistical difference between the RJB and SS bandage/splint constructs in regards to deflection distance and angle supports the hypothesis the SS bandage would provide adequate and similar stabilization. The significantly increased sub-bandage pressures obtained with the single stack bandage were within previously published range of pressures tolerated by horses and would likely result in improved hemostasis and reduction of edema. A limitation of the study is testing of the limbs was performed under a constant bending force in one place, versus cyclical loading in multiple planes as would be expected in a horse at the walk. Additionally, cadaver limbs were used for the study precluding the ability to evaluate clinical significance of bandage pressures, however ex vivo testing is important prior to in vivo work. Additionally the study population was 8 pairs of limbs providing low power, however lack of statistical difference supports the hypothesis. This work provides objective ex vivo data analyzing two commonly used bandages in equine practice for emergency fracture stabilization. The data supports our hypothesis that a single stack bandage could be utilized in field situations where a Robert Jones bandage may not be an option due to either finances, availability of materials, or safety of the situation. In addition, further work would be warranted to determine the optimal sub-bandage pressure of an equine bandage.

Acknowledgments. Would like to acknowledge Sonya Britt-Lutter for help with statistics, Katherine Neumann for help with the data collection, and Dylan Lutter for financial support through research funds.

Faculty/Staff Poster Presentations

Role of S1 N-terminal Domain Amino Acid Differences Among ArkDPI Infectious Bronchitis Virus Vaccine Subpopulations in Differential Binding to Chicken Tissues and Selection in Chickens

Vicky L. van Santen, Fatma E. Eldemery, Kellye S. Joiner

Department of Pathobiology, College of Veterinary Medicine, Auburn University, AL

Introduction. Infectious bronchitis virus (IBV) is a coronavirus that causes economic losses in the broiler and layer industries and is controlled by vaccination. Commercial attenuated ArkDPI-derived IBV vaccines contain subpopulations that are rapidly selected in and persist in vaccinated chickens. The S1 amino acid (aa) sequences of vaccine subpopulations positively selected in chickens differ by as few as four aa from the major vaccine populations negatively selected in chickens. At three of these four amino acid positions, ArkDPI-like S1 aa sequences of IBV identified in 80-98% of clinical samples match ArkDPI vaccine subpopulations selected in chickens, suggesting that these differences in S1 play a role in selection of vaccine subpopulations in chickens. Consistent with this hypothesis, we previously demonstrated that recombinant S1 protein representing the selected vaccine subpopulation C2, differing by only four aa from the major vaccine population (V), binds with higher affinity than V-S1 to chicken respiratory epithelium. We explore the effect of the two of these amino acid changes that fall within the S1 N-terminal domain (NTD) on binding to relevant chicken tissues.

Methods. Protein histochemistry using strep-tagged, soluble, trimeric recombinant spike proteins produced in mammalian cells.

Results. We show that the NTD (aa 19-279) of C2-S1 is necessary and sufficient for binding to these tissues. Neither a shorter NTD (aa 19-137), nor the S1-C-terminal domain (aa 259-538), nor S1 lacking aa 19-137 bound to any tissues tested. Surprisingly, S1-NTD binds chicken respiratory epithelium with higher affinity than complete S1. Like their S1s, C2-S1-NTD, which differs by only two aa from V-S1-NTD, binds with higher affinity than V-S1-NTD to respiratory epithelium. Binding assays with V-S1-NTD containing each of these two changes separately indicated that either aa change alone is sufficient to increase binding to levels equivalent to C2-S1-NTD. This was the case both for numerous chicken tissues and chorioallantoic membrane from 11 d chicken embryos. This contrasts with previous findings of others that changing aa 43 in the ArkDPI S1 to that of C2 destroyed, rather than increased, binding to chorioallantoic membrane. Thus the effect of individual amino acid differences on binding can possibly be influenced by the presence of the S1-CTD.

Conclusions. Taken together, our results suggest that the ability of the receptor binding site(s) in the S1-NTD to bind chicken tissues is influenced by its context. Because the capacity to elicit effective neutralizing antibodies is likely related to the ability to bind receptors, this further suggests that the context of receptor binding sites might be an important consideration in designing recombinant vaccines.

Acknowledgments. We are grateful to Cynthia Hutchinson for excellent technical assistance. This work was supported by Alabama Animal Health & Disease Research. Fatma Eldemery was supported by the Egyptian Cultural and Educational Bureau, Washington, DC.

Bisphenol A and bisphenol S regulation of steroid hormone secretion in the rat testis

Rachel Knight, Bamidele O. Jeminiwa, Kodye L. Abbot, Satyanarayana R. Pondugula and Benson T. Akingbemi

Department of Anatomy, Physiology and Pharmacology, College of Veterinary Medicine, Auburn University AL 36849

Introduction: Bisphenol S (BPS) is an analog of bisphenol A (BPA), which is used in consumer products due to its superior thermal stability. BPS is considered a safe replacement chemical for BPA but only a small number of studies have examined the effects of BPS in mammals. We have now employed a pre-pubertal exposure paradigm to compare BPA and BPS effects on serum sex steroid hormone concentrations in young growing rats.

Methods: In the first experiment, weanling 21 day-old Long-Evans male rats (n=6) were fed BPA or BPS in drinking water *ad libitum* at 0, 5, 10, 15 and 20 µg/L for 14 days, i. e, until 35 days post-partum, when exposure to chemicals was terminated. Chemicals were fed in water to avoid activation of the hypothalamus-pituitary-adrenal axis, a common gavage effect. Within 24 h of postnatal day 35, animals were sacrificed to collect blood and obtain serum to measure serum testosterone (T) concentrations using a tritium-labeled radioimmunoassay (RIA).

Results: In the first experiment, serum T concentrations were similar in control and DMSO groups of animals (2.5±0.6 versus 2.2±0.6 ng/mL), but exposure to BPA at 20 µg/L of drinking water decreased serum T levels (2.5±0.6 versus 1.2+0.2 ng/mL; $p<0.05$). Exposure to BPS at the 10 µg/L concentration decreased serum T concentrations compared to levels measured in control animals (0.9±0.2 versus 0.6±0.1 ng/mL; $p<0.05$), but this effect was not seen in other BPS-exposed animals ($p>0.05$). In the second experiment, male rats were fed BPA and BPS at 10 and 20 µg/L of drinking water. From 21 to 35 days of age there was a decrease ($p<0.05$) in serum T concentration in animals treated with both BPA and BPS at the 20 µg/L concentration. Measurement of testosterone secretion by testicular explants showed that exposure to BPA at 20 µg/L decreased basal testosterone production while it increased in LH-stimulated testosterone production at the 10 µg/L concentration

Conclusions: Together, these observations demonstrated that BPA and BPS have similar inhibitory effects on gonadal steroidogenesis albeit in a dose-dependent manner. These findings reinforce the view that exposures of the population to environmental chemicals have the potential to disrupt reproductive activity and impair reproductive health.

Acknowledgements: This study was supported in part by Animal Health and Disease Research Program, Auburn University College of Veterinary Medicine.

Nanobody based immune checkpoint inhibitor for immunotherapy of canine cancers

Jonathan Marable[1], Damien Ruiz[1] and Maninder Sandey[1]
[1]Department of Pathobiology, College of Veterinary Medicine, Auburn University, AL

Recent advances in cancer immunotherapy including the use of immune checkpoints inhibitors have dramatically improved the outcomes for human patients with advanced melanoma. During cancer progression, tumor cells co-opt immune checkpoints to avoid immune surveillance and antitumor immunity. To date, the FDA has approved four immune checkpoint inhibitors that block PD-1/PDL-1 or CTLA-4/B7.2 pathways for advanced and metastatic human cancers including melanoma. Monoclonal antibodies blocking the immune checkpoints have shown remarkable success and improved clinical outcome for human cancer patients. However, adoption of immunotherapy for canine patients has been slow due to the lack of effective therapeutic antibodies. *Thus, the primary goal of the project is to develop antibody-based therapeutics for the treatment of canine cancers.* Camelid heavy chain-only antibodies are composed of a single heavy chain and bind to antigens in the absence of a light chain. Nanobodies (representing the variable domain of Camelid Heavy chain only antibodies) are small in size (~15kDa), highly soluble and stable in extreme pH and thermal conditions. They exhibit excellent tissue penetration and biodistribution due to their small size. Several studies have shown that nanobodies can delay tumor growth, inhibit angiogenesis and perform at the same level as their corresponding mAbs. *Thus, the primary goal of this project is to identify and characterize nanobodies that can bind canine PD-1 and inhibit its interaction with PD-L1.* To identify nanobodies targeting canine PD-1, we used a yeast surface display platform that expresses $1X10^8$ unique nanobodies on the surface of yeast cells. The commercially purchased canine PD-1 protein was labeled with either biotin or Alexa flour-647 fluorophores using the microscale protein labelling kit (ThermoFisher). After preclearing, canine PD-1 specific binders were enriched over two rounds of MACS selection by staining the yeast successively with Alexa Flour-647- or biotin-labelled canine PD-1 protein. To enrich for high-affinity binders, lower concentration of labelled protein was used for iterative round of selection. After two rounds of selection, single yeast clones were isolated, stained with Alexa Fluor 647-labeled canine PD-1 protein, and analyzed by flow cytometry to confirm their ability to bind to the canine PD-1 protein. The recombinant plasmids encoding the nanobody sequences were isolated from the specific canine PD-1 binders, amplified and sequenced to know the nanobody sequences. Induction of the yeast library with galactose resulted in expression of nanobodies on 26-31% of the yeast cells. After two round of MACS selection, approximately 12.0 % of the yeast cells strongly bound to the canine PD-1 protein. After successful enrichment of canine PD-1 binder, a FACS sort was performed, and individual yeast cells were grown as clonal populations in 96-well plate. Twelve clones were randomly selected for further analysis. Following galactose induction, most yeast clones (11/12) bound the canine PD-1 protein. Nanobody sequences from the ten yeast clones that bind strongly to the canine PD-1 protein have nanobodies belonging to three families containing 7 (6), 11 (2) or 15 (2) amino acids in the CDR3 region. In the future experiments, we will clone, express and purify nanobodies for in-depth characterization.

Methods for Isolation of RNA from Canine Osteosarcoma

Rebecca Nance[1], Payal Agarwal[2], Dmytro Starenki[3], Brad Matz[4], Jey Koehler[2], Maninder Sandey[2], Paulina Platten[1,5], Damien Ruiz[2], Abdul Sajib[2], Bruce Smith[1,2]

[1]Scott-Ritchey Research Center, College of Veterinary Medicine, Auburn University
[2]Department of Pathobiology, College of Veterinary Medicine, Auburn University
[3]HudsonAlpha Institute for Biotechnology, Huntsville
[4]Department of Clinical Sciences, College of Veterinary Medicine, Auburn University
[5]College of Veterinary Medicine, Texas A&M

Introduction. The heterogeneous nature of cancer, both between and within individuals, has catalyzed the potential for precision designed, patient-specific cancer treatment. Evaluation of the differentially expressed RNA profiles between functionally "normal" cells and the cancerous mass originating from the same tissue type provides a powerful opportunity to identify potential targets for developing and customizing cancer therapies. Osteosarcoma (OSA) is the most frequent bone tumor in dogs and is locally and systemically aggressive. Isolation of RNA from tumor has been well established. In contradistinction, isolation of RNA from bone presents a unique challenge due to the presence of bone marrow as well as the hypocellular, brittle, and mineralized bone matrix, which makes homogenizing the tissue difficult. With the exception of a single murine study, current methods for isolating RNA from bone do not take into account the contaminating bone marrow RNA, which has an RNA profile distinct from that of bone, thereby skewing the transcriptome expression profile. This study was designed to establish a protocol to effectively isolate RNA from normal canine bone using the phalanges, sans contamination from other tissue types, in addition to RNA isolation from the patient's OSA mass for downstream transcriptomic analysis.

Methods. Phalanx bone and tumor specimens were obtained from six dogs undergoing routine limb amputation for osteosarcoma at the Auburn University College of Veterinary Medicine. Bone marrow was removed by a combination of centrifugation and flushing. RNA was isolated from bone using an altered homogenization procedure followed by an adapted Tri-Reagent protocol. Tumor RNA was isolated using the classical Tri-Reagent protocol.

Results. Histological staining of processed versus unprocessed bone samples indicated complete removal of bone marrow. The integrity of extracted RNA was evaluated using the RNA Integrity Number (RIN), and purity and concentration was assessed using the absorbance ratios 260/280 and 260/230.

Conclusions. We have demonstrated an adapted protocol for isolation of RNA from canine phalanges independent of bone marrow which successfully yields sufficient quantity and quality of RNA for transcriptomic sequencing. This protocol is essential for extracting RNA to compare with that of OSA for downstream analysis of varied gene expression to identify potential unique targets for precision medicine.

Acknowledgments. Scott-Shockley Foundation funding, AURIC MGP grant funding, Dr. Bruce Smith and lab team.